NAVAL POSTGRADUATE SCHOOL
Monterey, California

THESIS

PASSIVE DETERMINATION OF TEMPERATURE
AND
RANGE USING SPECTRAL BAND MEASURE-
MENTS
OF PHOTON EMITTANCE

by

Shinji Hirakawa

September 1991

Thesis Advisor Ronald J. Pieper

Approved for public release; distribution is unlimited.

T257863

Unclassified

ecurity classification of this page

REPORT DOCUMENTATION PAGE

1a Report Security Classification: Unclassified			1b Restrictive Markings
2a Security Classification Authority			3 Distribution/Availability of Report: Approved for public release; distribution is unlimited.
2b Declassification/Downgrading Schedule			
4 Performing Organization Report Number(s)			5 Monitoring Organization Report Number(s)
6a Name of Performing Organization: Naval Postgraduate School	6b Office Symbol (*if applicable*): 3A		7a Name of Monitoring Organization: Naval Postgraduate School
6c Address (*city, state, and ZIP code*): Monterey, CA 93943-5000			7b Address (*city, state, and ZIP code*): Monterey, CA 93943-5000
8a Name of Funding/Sponsoring Organization	8b Office Symbol (*if applicable*)		9 Procurement Instrument Identification Number
8c Address (*city, state, and ZIP code*)			10 Source of Funding Numbers: Program Element No / Project No / Task No / Work Unit Accession No

11 Title (*Include security classification*): PASSIVE DETERMINATION OF TEMPERATURE AND RANGE USING SPECTRAL BAND MEASUREMENTS OF PHOTON EMITTANCE

12 Personal Author(s): Shinji Hirakawa

13a Type of Report	13b Time Covered	14 Date of Report (*year, month, day*)	15 Page Count
Master's Thesis	From To	September 1991	87

16 Supplementary Notation: The views expressed in this thesis are those of the author and do not reflect the official policy or position of the Department of Defense or the U.S. Government.

17 Cosati Codes			18 Subject Terms (*continue on reverse if necessary and identify by block number*)
Field	Group	Subgroup	passive ranging, temperature determination, photon emittance, spectral band measurements

19 Abstract (*continue on reverse if necessary and identify by block number*)

The established concept of temperature determination from dual spectral band radiometric measurement is analyzed for the case that the measurement device is sensitive to total photon emittance rather than radiant emittance. A temperature dependent ratio of measurements is calculated for two distinct spectral bands using a black body distribution. It is shown that, if the bands are *not self contained,* then there exists a one-to-one correspondence between temperature and ratio.

A prototype algorithm is proposed and tested which demonstrates the feasibility of extracting both the temperature and range by using three distinct spectral band measurements. The model assumes nonhomogeneous, wavelength-dependent atmospheric attenuation. The target and sensor systems each have an arbitrary location in a vertical plane relative to the earth. In the computer simulations, LOWTRAN data was used.

20 Distribution/Availability of Abstract	21 Abstract Security Classification	
☒ unclassified/unlimited ☐ same as report ☐ DTIC users	Unclassified	
22a Name of Responsible Individual: Ronald J. Pieper	22b Telephone (*include Area code*): (408) 646-2101	22c Office Symbol: EC/Pr

DD FORM 1473,84 MAR 83 APR edition may be used until exhausted
All other editions are obsolete

security classification of this page

Unclassified

Approved for public release; distribution is unlimited.

Passive determination of temperature and range using spectral band measurements of photon emittance

by

Shinji Hirakawa
Lieutenant, Japan Maritime Self Defense Force
B.S.equivalent, The National Defense Academy,Japan, 1983

Submitted in partial fulfillment of the
requirements for the degree of

MASTER OF SCIENCE IN SYSTEMS ENGINEERING

from the

NAVAL POSTGRADUATE SCHOOL
September 1991

ABSTRACT

The established concept of temperature determination from dual spectral band radiometric measurement is analyzed for the case that the measurement device is sensitive to total photon emittance rather than radiant emittance. A temperature dependent ratio of measurements is calculated for two distinct spectral bands using a black body distribution. It is shown that, if the bands are *not self contained*, then there exists a one-to-one correspondence between temperature and ratio.

A prototype algorithm is proposed and tested which demonstrates the feasibility of extracting both the temperature and range by using three distinct spectral band measurements. The model assumes nonhomogeneous, wavelength-dependent atmospheric attenuation. The target and sensor systems each have an arbitrary location in a vertical plane relative to the earth. In the computer simulations, LOWTRAN data was used.

/R613
H57745
C.1

TABLE OF CONTENTS

I. INTRODUCTION 1
A. REVIEW OF PRIOR WORK 1
B. OVERVIEW OF THE THESIS 3

II. BACKGROUND 5

III. DUAL SPECTRAL BAND MEASUREMENTS FOR TEMPERATURE DETERMINATION 9
A. NON-OVERLAPPING CASE 11
B. PARTIALLY OVERLAPPING AND COMMON BAND LIMIT CASE . 15
C. TOTALLY CONTAINED SPECTRAL-BAND CASE 16
D. RATIO CALCULATION FOR PHOTON EMITTANCE 17
E. DISCUSSION OF COMPUTER RESULTS 18

IV. A GENERAL MODEL FOR TEMPERATURE DETERMINATION VIA DUAL SPECTRAL BAND MEASUREMENTS 27
A. EMISSIVITY 27
B. ATMOSPHERIC TRANSMITTANCE 28
C. DETECTOR RESPONSIVITY 29
D. COMPUTER SIMULATION OF TEMPERATURE DETERMINATION 31
1. Discussion of the computer simulations 32

V. THERMAL RANGING TECHNIQUE 38
A. RANGING FOR KNOWN TEMPERATURE CONDITION WITH HOMOGENEOUS ATMOSPHERIC CONDITIONS 39
B. RANGING FOR UNKNOWN TEMPERATURE WITH HOMOGENEOUS ATMOSPHERIC CONDITIONS 41
C. RANGING FOR UNKNOWN TEMPERATURE WITH INHOMOGENEOUS ATMOSPHERIC CONDITIONS 42

VI. CONCLUSIONS 61

APPENDIX A. DERIVATIVE OF $\mathscr{R}$ WITH RESPECT TO T 63

APPENDIX B. ASYMPTOTIC APPROXIMATION FOR RATIO CALCULATION 67
A. FOR LARGE ALPHA 67
B. FOR SMALL ALPHA 69

APPENDIX C. ALGORITHM TO CALCULATE THE RATIO OF PHOTON EMITTANCE 72

APPENDIX D. ALGORITHM TO CALCULATE THE RATIO OF OUTPUT VOLTAGE AT THE DETECTOR 73

APPENDIX E. MODEL FOR PASSIVE RANGE AND TEMPERATURE DETERMINATION 74
A. MAIN ALGORITHM 74
B. LOWTRAN DATA GENERATION 75
C. LAYER (SUBROUTINE) 76
D. MEASURED RATIO PREDICTOR 77

LIST OF REFERENCES 78

INITIAL DISTRIBUTION LIST 80

LIST OF FIGURES

Figure 1. graphical representation of possible band combination 8
Figure 2. Plot of $f(\psi)$ and $\beta g(\psi)$ for $\beta = 1,2,...,5$ 19
Figure 3. Nonoverlapping case. 20
Figure 4. Partially overlapping case or common band limit case 21
Figure 5. Example of totally contained case (normalized ratio) 22
Figure 6. Example of totally contained case (normalized ratio) 23
Figure 7. Example of the non-overlapping case 24
Figure 8. Example of the partially overlapping case 25
Figure 9. Example of the totally contained case 26
Figure 10. Atmospheric transmittance for 1962 U.S. standard atmosphere 33
Figure 11. Example of the emissivity (arbitrary chosen) 34
Figure 12. The ratio of output voltages for nonoverlapping case 35
Figure 13. The ratio of output voltages for partially overlapping case 36
Figure 14. The ratio of output voltages for totally contained band case 37
Figure 15. Definition of vertical line from the earth through the receiver 50
Figure 16. Ideal ratio curves 51
Figure 17. Definition of layers in atmosphere 52
Figure 18. Layer of the atmosphere 53
Figure 19. Geometry of ranging 54
Figure 20. Geometry of ranging (cosine law) 55
Figure 21. Measured ratio curves 56
Figure 22. Graphical solution of range and temperature 57
Figure 23. Initial guess range (the worst case) 58
Figure 24. Error of range determination 59
Figure 25. Error of temperature determination 60

I. INTRODUCTION

A. REVIEW OF PRIOR WORK

In the photon detection process electromagnetic radiation causes three kinds of mechanism such as photon effects, thermal effects, and wave interaction effects [Ref. 1]. The focus of the remaining discussion will be confined to the first two effects which cover the majority of applications involving the detection of thermal radiation. One common photon effect is photoconductivity. Photoconductivity is observed in semiconductors and characterized by photon energy and energy gap. One common device which uses a thermal effect is the bolometer. Bolometers can be made of any material which has a temperature-dependent resistance. This effect is characterized by the change of resistance from the heating effect of incident radiation. Therefore, Plank's equation for radiant emittance can only be applied directly to thermal effects. Although some devices have a detection mechanism based on the thermal heating effects due to radiation, this is not true of semiconductor-based detectors. Semiconductors devices are characterized by an energy gap. Only photons with energies greater than this gap can produce electron hole pairs which contribute to the detected signal. The excess photon energy is dissipated as heat [Ref. 2] and therefore does not contribute to the electrical signal generated. Specifically the integrated spectral emittance [Ref. 3], i.e., photon flux, is a more appropriate signal indicator than the radiant emittance for measurements based on semiconductor devices.

R.B. Johnson and E.E. Branstetter presented a numerical method for the integration of Plank's equation [Ref. 4]. Johnson derived an approximated equation for effective radiant sterance [Ref. 5]. Normalization of spectral bandwidth, for convenience in analysis, was provided by F.E. Nicodemus [Ref. 6]. Based on Plank's equation for ra-

diant emittance, M.H. Horman presented the technique for temperature determination using the ratio of output from two bands [Ref. 7]. On the other hand, analysis of the dual spectral band temperature measurement for devices based on the photon effects has not been developed.

One standard method for the determination of the gray-body emissivity and the temperature of an object is based on two separate narrowband radiometric power measurements. In combination with Plank's radiation equation for a gray-body, two narrowband measurements are sufficient to produce a unique value for both temperature and emissivity. For practical reasons, such as improvement of signal-to-noise ratio, most instrumentation take measurements over bands which are too wide to be considered narrowband. In this more general situation the question of uniqueness of temperature requires more careful consideration. This issue has been recently analyzed for the distribution based on a Plank's spectral radiant emittance [Ref. 8]. The authors developed an analysis based on the evaluation of the ratio ($\mathscr{R}$) of two measurements of the integrated power distribution over separate bands. Three cases, nonoverlapping bands, partially overlapping bands and totally overlapping bands, were considered. The analytical investigation demonstrated that the last case does not always generate a one-to-one correspondence between the ratio $\mathscr{R}$ and the temperature.

For the passive ranging technique, P.J. Ovrevo and R.C. Wood presented the method using absorption property of the atmosphere [Ref. 9], and J.R. Jenness, Jr., and F.J. Shimukonis proposed the principle of passive ranging using the ratio of the signals in narrow spectral bands received [Ref. 10].

For optical properties of the atmosphere, R.A. McClatchey and others described effects of index of refraction in the atmosphere [Ref. 11: pp. 41]. It was found that transmission factors are affected by no more than 1 - 2 % if refraction is included in the calculation.

B. OVERVIEW OF THE THESIS

Chapter I is the introduction and covers both a review of relevant literature and a thesis overview. In the interest of keeping this thesis fairly self-contained, Chapter II provides a brief technical description of essential background preliminaries. In Chapter III, effects due to atmospheric attenuation and detector responsivity are ignored. Using dual spectral measurements, it is shown that it is possible to uniquely determine a target's temperature if the detector bands are not 100 % overlapping. Specifically, the ratio of the dual spectral band measurements is shown to exhibit a mathematically predictable one-to-one correspondence with the temperature, as long as the bands are not totally contained within the other.

In Chapter IV, a numerical program for calculating a spectral band measurement without the assumption of constant atmospheric attenuation and detector responsivity is discussed and tested In the process of this development, a novel definition for a "responsivity", applicable to devices sensitive to photon emittance, has been introduced. If the effects of atmospheric attenuation on the dual spectral band measurement are not equivalent, then the ratio scheme for temperature determination, discussed in Chapter III, is not applicable. It is precisely under these conditions that by using three distinct bands both the temperature and the range can be determined.

In Chapter V, a prototype algorithm is discussed, which demonstrates the feasibility of obtaining both the temperature and the range of a target using three distinct spectral band measurements. Complications introduced by not assuming constant altitude of the target-to-sensor trajectory are addressed. LOWTRAN data was also used here to characterize atmospheric attenuation. Conclusions for the thesis are presented in Chapter VI. In order to not obscure the main points of the thesis, the extensive mathematical derivations have been relegated to appendices. Both Appendix A and Appendix B fit this description. Appendix C, Appendix D and Appendix E have been created for those

readers who are interested in an algorithmic description of programs used in the computer simulation.

II. BACKGROUND

In this chapter, an alternate approach based on photon emittance rather than radiant emittance is applied. This kind of treatment is appropriate for photovaltaic or photoconductive semiconductor devices but not radiometers. First, a few basic assumptions need to be presented. The discussion starts from the ideal case with the following preliminary assumptions [Ref. 8: pp. 1256]:

- opaque object
- Lambertian surface
- object in thermal equilibrium
- spectrally constant emissivity (gray body)
- photon emittance derived from Plank's radiation law
- unity spectral transmittance of intervening media between the object and measuring instrument.

Plank's radiation law gives the spectral radiant emittance, which is given by [Ref. 3: pp. 35]:

$$W_\lambda(\lambda,T) = \frac{2\pi\varepsilon(\lambda)hc^2}{\lambda^5[exp(hc/\lambda kT) - 1]} \quad [W \cdot cm^{-2} \cdot \mu m^{-1}], \tag{2.1}$$

where $\varepsilon(\lambda)$ is the spectral emissivity, h is Plank's constant, λ is the wavelength, c is the speed of light, k is Boltzmann's constant, and T is the object's temperature. In this section, since the emissivity is assumed to be spectrally constant, $\varepsilon(\lambda)$ is denoted as ε.

The photon emittance is derived from (2.1) dividing by hc/λ, which is the energy associated with one photon [Ref. 3: pp. 38]. Therefore photon emittance is the flux related to the number of photons. The resultant photon emittance equation is obtained as

$$Q_\lambda = \frac{2\pi\varepsilon c}{\lambda^4[exp(hc/\lambda kT) - 1]} \quad [photons \cdot s^{-1} \cdot cm^{-2} \cdot \mu m^{-1}] \tag{2.2}$$

The integral of (2.2) over some band limits gives the photon emittance in the bands. The photon emittance within the spectral band limits $[\lambda_1, \lambda_2]$ is given by

$$Q(\lambda_2, \lambda_1, T) = \int_{\lambda_2}^{\lambda_1} Q_\lambda(\lambda, T)d\lambda \tag{2.3}$$

From the assumptions, emissivity is assumed to be spectrally constant. Therefore photon emittance for a gray body is simply expressed as photon emittance for a black body multiplied by a constant emissivity and given by

$$Q_\lambda = \varepsilon Q_{BB_\lambda}. \tag{2.4}$$

From (2.3), it follows from (2.4) that

$$\begin{aligned} Q(\lambda_2, \lambda_1, T) &= \varepsilon \int_{\lambda_2}^{\lambda_1} Q_{BB_\lambda}(\lambda, T)d\lambda \\ &= \varepsilon Q_{BB}(\lambda_2, \lambda_1, T), \end{aligned} \tag{2.5}$$

where $\lambda_2 < \lambda_1$ and $Q_{BB_\lambda}(\lambda, T)$ is the spectral photon emittance for a blackbody $[\varepsilon(\lambda) = 1]$.

It has been shown that the temperature of an object can be determined by taking a ratio of measured radiant emittance of an object in each of two spectral bands. [Ref. 8: pp. 1256] In Chapter II and Chapter III, this concept is applied in a similar manner except the assumption is made that a ratio is formed from the measured photon emittance. Let the two spectral bands be denoted as $[\lambda_2, \lambda_1]$ and $[\lambda_4, \lambda_3]$. Let the ratio for photon emittance be defined as

$$\mathcal{R}_p(\lambda_1, \lambda_2, \lambda_3, \lambda_4, T) = \frac{Q(\lambda_2, \lambda_1, T)}{Q(\lambda_4, \lambda_3, T)}. \tag{2.6}$$

Since from the assumption, emissivity is uniform over the spectral band, emissivity is cancelled out, and the ratio becomes the ratio of the photon emittances associated with a black body, as shown by

$$\mathcal{R}_p(\lambda_1, \lambda_2, \lambda_3, \lambda_4, T) = \frac{Q_{BB}(\lambda_2, \lambda_1, T)}{Q_{BB}(\lambda_4, \lambda_3, T)}. \tag{2.7}$$

This implies that $\mathcal{R}_p$ is a function of the object's temperature T only and the ratio can indicate the object temperature. When the dual spectral-band photon emittance method is used, it is critical to know that the ratio $\mathcal{R}_p$ and the temperature have a one-to-one correspondence. For this purposes, three general cases of spectral bands which cover all possibilities are considered. The possible cases are [Ref 8: pp. 1256]

1. non-overlapping bands (Figure 1a),
2. partially overlapping bands and common band limits (Figure 1b,c), and
3. totally contained band (Figure 1d).

These three cases are presented graphically in Figure 1. In the following two chapters the validity of temperature determination based on dual spectral photon emittance for the ideal case is discussed.

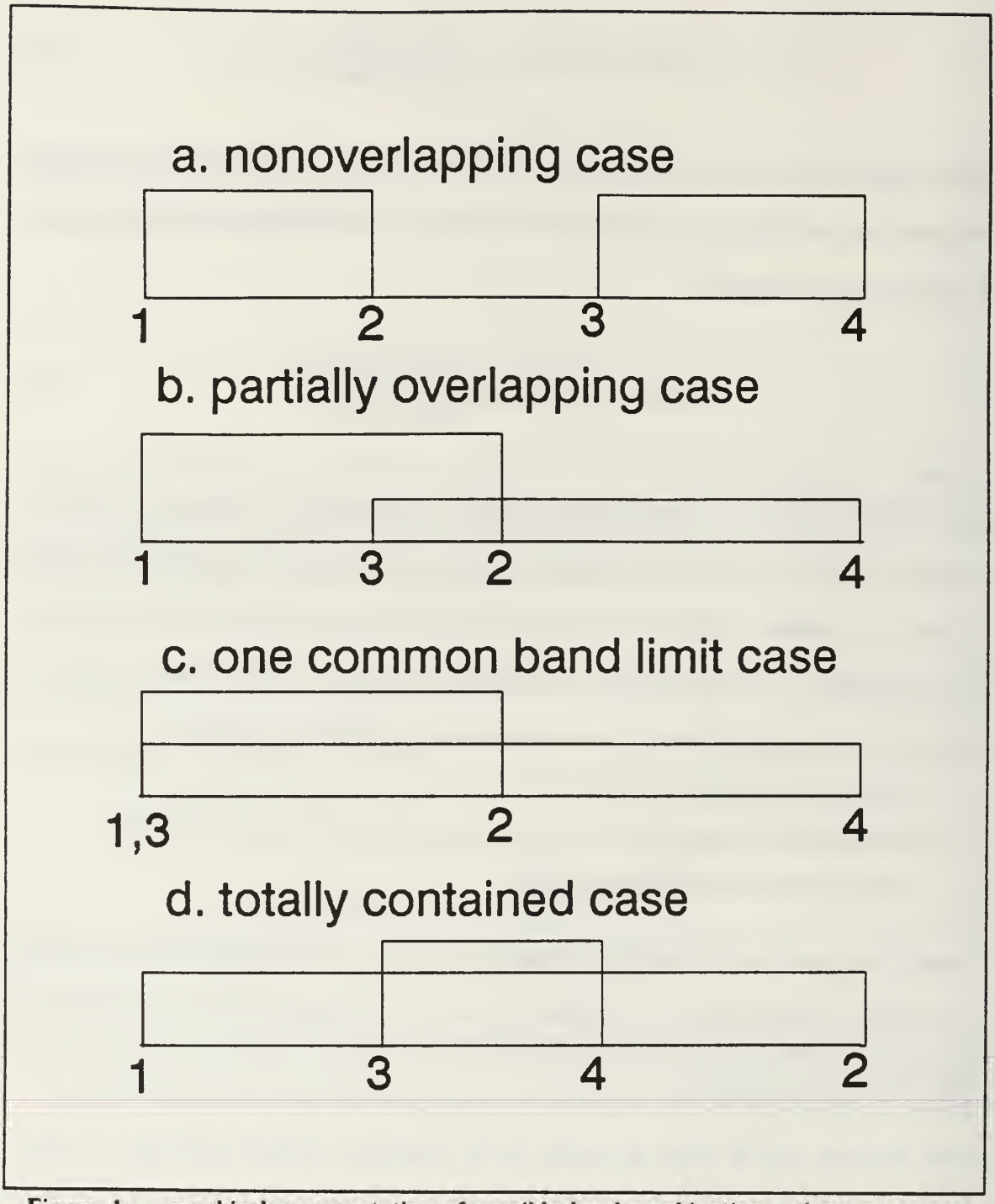

Figure 1. graphical representation of possible band combination: three cases are nonoverlapping, partially overlapping, and totally contained.

III. DUAL SPECTRAL BAND MEASUREMENTS FOR TEMPERATURE DETERMINATION

In this section the ratio of photon emittance defined in (2.6) is considered for the various cases discussed at the end of Chapter II. In order to validate the dual spectral bands method, it is required to show one-to-one correspondence between the ratio and the temperature of the object. For this purpose, the derivative of the ratio of band limited photon fluxes, $\mathcal{R}_p$ in (2.7), with respect to temperature is performed. If the ratio of photon emittance $\mathcal{R}_p$ is proved to be either strictly increasing or strictly decreasing function with respect to temperature, i.e., either $\partial\mathcal{R}_p/\partial T > 0$ or $\partial\mathcal{R}_p/\partial T < 0$ for all T, then the ratio of photon emittances and the temperature exhibit a one-to-one correspondence. It follows that this approach is potentially applicable to the temperature determination of grey bodies.

To simplify the integral of (2.2) , the variables of integration in photon emittance $Q(\lambda_i, \lambda_j, T)$ are replaced by the dimensionless parameters [Ref. 8: pp. 1257]

$$\psi = \frac{hc}{\lambda k T}, \tag{3.1}$$

and

$$\alpha = \frac{T_r}{T}, \tag{3.2a}$$

where T_r is an arbitrary reference temperature. By prior convention [Ref. 8: pp. 1257], it is chosen to be

$$T_r = \frac{hc}{\lambda_1 k}, \tag{3.2b}$$

where λ_1, as introduced in Chapter II, is the highest wavelength in spectral band 1. Using (3.2b) as a reference temperature in (3.1), the spectral band limits of ψ are given by:

$$x_i = \frac{hc}{\lambda_i k T_r} \tag{3.3}$$

where λ_i is one of the spectral band limits [Ref. 8: pp. 1257]. After substitutions into (2.5), the new representation for the photon emittance is given by

$$Q(\lambda_i, \lambda_j, T) = 2\pi\varepsilon k^3 T^3 c^{-2} h^{-3} \int_{\alpha x_j}^{\alpha x_i} g(\psi) d\psi, \tag{3.4}$$

where [Ref. 8: pp. 1257]

$$g(\psi) = \frac{\psi^2}{\exp(\psi) - 1}. \tag{3.5}$$

The ratio of photon emittance is obtained as

$$\mathcal{R}_p = \frac{\int_{\alpha}^{\alpha x_2} g(\psi) d\psi}{\int_{\alpha x_3}^{\alpha x_4} g(\psi) d\psi} \tag{3.6}$$

and the derivative of the ratio of photon emittance signals (3.6) with respect to temperature comes out to be

$$\frac{\partial \mathcal{R}_p}{\partial T} = \frac{1}{T} \frac{\int_{\alpha}^{\alpha x_2} f(\psi) d\psi \int_{\alpha x_3}^{\alpha x_4} g(\psi) d\psi - \int_{\alpha}^{\alpha x_2} g(\psi) d\psi \int_{\alpha x_3}^{\alpha x_4} f(\psi) d\psi}{\left[\int_{\alpha x_3}^{\alpha x_4} g(\psi) d\psi\right]^2}, \tag{3.7}$$

where

$$f(\psi) = \frac{\exp(\psi)\psi^3}{[exp(\psi) - 1]^2}. \tag{3.8}$$

(The derivation of (3.7) is in Appendix A.) To simplify the expression of (3.7), the following operator is defined [Ref. 8: pp. 1257].

$$[a,b](1, x_2, x_3, x_4, \alpha) = \int_{\alpha}^{\alpha x_1} a(\psi)d\psi \int_{\alpha x_3}^{\alpha x_4} b(\psi)d\psi - \int_{\alpha}^{\alpha x_1} b(\psi)d\psi \int_{\alpha x_3}^{\alpha x_4} a(\psi)d\psi \tag{3.9}$$

Then the ratio becomes

$$\frac{\partial \mathcal{R}_p}{\partial T} = \frac{1}{T} \frac{[f,g](1, x_2, x_3, x_4, \alpha)}{\left[\int_{\alpha x_3}^{\alpha x_4} g(\psi)d\psi\right]^2}. \tag{3.10}$$

Since the denominator of (3.10) is always positive, the sign of $\partial \mathcal{R}_p / \partial T$ is determined by the sign of the operator [f,g]. It is necessary to show that the sign of [f,g], which is the sign of (3.10), does not change with α, or equivalently with temperature. The temperature dependence of [f,g] appears only in α, which can be seen in the limits of integration. The integrands do not have an explicit dependence on temperature.

A. NON-OVERLAPPING CASE

In order to prove that the sign of [f,g] is fixed over the domain of α, several properties of $f(\psi)$ and $g(\psi)$ are required. They are [Ref. 8: pp. 1257]

1. $f(0) = g(0) = 0$
2. $0 < g(\psi) < f(\psi)$ for $\psi > 0$
3. $\lim_{\psi \to \infty} f(\psi) = \lim_{\psi \to \infty} g(\psi) = 0$
4. For $\beta > 1, f(\psi) - \beta g(\psi)$ has exactly one root on the interval $\psi \in (0, \infty)$.

The discussion to follow will clarify the significance of these requirements. Graphical representation is useful to clarify these properties and it is shown in Figure 2. This figure is especially useful for visualization of the fourth property. For values of $\beta > 1$, it is obvious that $f(\psi)$ crosses $\beta g(\psi)$ exactly once. A more formal discussion of the four properties is provided in the next paragraph.

The first property is proven by using l'Hopital's rule. In order to prove the second property, define

$$P(\psi) \equiv \frac{f(\psi)}{g(\psi)}. \tag{3.11a}$$

which by direct substitution from (3.5) and (3.8) is given by

$$P(\psi) = \frac{\psi}{1 - \exp(-\psi)}. \tag{3.11b}$$

It then can be shown that $P(\psi) > 1$ for $\psi > 0$. This follows from the derivative of P(ψ), which is :

$$\frac{dP(\psi)}{d\psi} = \frac{1 - \exp(-\psi) - \psi \exp(-\psi)}{(1 - \exp(-\psi))^2}. \tag{3.12a}$$

After expanding (3.12a), it is clear that :

$$\frac{dP(\psi)}{d\psi} = \frac{1}{1 - \exp(-\psi)} - \frac{\psi \exp(-\psi)}{(1 - \exp(-\psi))^2} > 0 \tag{3.12b}$$

which follows from the observation that the second term in the expansion is smaller in magnitude. Also, by direct application of l'Hopital's rule on (3.11b), $\lim_{\psi \to 0^+} P(\psi) = 1$. These two results imply that $P(\psi) > 1$. Thus $f(\psi) > g(\psi)$. Consequently, after noting that both $f(\psi)$, as given in (3.8), and $g(\psi)$, as given in (3.5), are strictly positive, property two

follows. The third property is simply proven by limit evaluation. For the fourth property, it is necessary to evaluate $f(\psi) - \beta g(\psi)$ given by

$$f(\psi) - \beta g(\psi) = \frac{\exp(\psi)\psi^3}{(\exp(\psi) - 1)^2} - \beta \frac{\psi^2}{\exp(\psi) - 1} \tag{3.13a}$$

which can be expressed as

$$f(\psi) - \beta g(\psi) = \frac{\psi^2}{\exp(\psi) - 1} \left(\frac{\psi \exp(\psi)}{\exp(\psi) - 1} - \beta \right). \tag{3.13b}$$

By noting (3.11b), it follows that

$$f(\psi) - \beta g(\psi) = \frac{\psi^2}{\exp(\psi) - 1} [P(\psi) - \beta]. \tag{3.13c}$$

Since $\lim_{\psi \to 0^+} Q(\psi) = 1$ and β is constrained to be greater than one, the quantity $f(\psi) - \beta g(\psi)$ satisfies, after reference to (3.11a), the inequality

$$f(\psi) - \beta g(\psi) < 0 \quad (\text{small } \psi) \tag{3.14a}$$

for sufficiently small ψ. Also since $\lim_{\psi \to 0^\infty} P(\psi) = \infty$, the inequality has to reverse for large enough ψ. In other words

$$f(\psi) - \beta g(\psi) > 0 \quad (\text{large } \psi). \tag{3.14b}$$

Since, from (3.12a), P(ψ) is a strictly increasing function, it is correct to conclude the inequality reversal can only occur once. Property 4 is therefore proven.

For the non-overlapping case represented on Figure 1a, there are only two sets of relations which can define the spectral bands (3.3):

$$1 < x_2 \leq x_3 < x_4, \tag{3.15a}$$

and

$$x_3 < x_4 \leq 1 < x_2. \tag{3.15b}$$

Relation (3.15a) is considered first. Motivated by the fourth property previously stated, let

$$\beta(\alpha) = \frac{f(\alpha x_2)}{g(\alpha x_2)}. \tag{3.16}$$

The quantities $f(\psi)$ and $\beta(\alpha)g(\psi)$ must cross each other only once at the value of ψ denoted as x_2. This is represented in Figure 3. The geometrical aspects of figures dictates the following relations for all values of α:

$$\int_{\alpha}^{\alpha x_2} f(\psi)d\psi < \int_{\alpha}^{\alpha x_2} \beta(\alpha)g(\psi)d\psi \tag{3.17a}$$

and

$$\int_{\alpha x_3}^{\alpha x_4} f(\psi)d\psi > \int_{\alpha x_3}^{\alpha x_4} \beta(\alpha)g(\psi)d\psi. \tag{3.17b}$$

Substitution (3.17a) and (3.17b) into (3.9) shows the operator [f,g] satisfies:

$$[f,g](1, x_2, x_3, x_4, \alpha) < \int_{\alpha}^{\alpha x_2} \beta(\alpha)g(\psi)d\psi \int_{\alpha x_3}^{\alpha x_4} g(\psi)d\psi - \int_{\alpha}^{\alpha x_2} g(\psi)d\psi \int_{\alpha x_3}^{\alpha x_4} \beta(\alpha)g(\psi)d\psi = 0$$

(3.18)

for all the values of α (3.2a). According to the brief description following (3.10), this proves that $\partial \mathcal{R}_p / \partial T < 0$ for all the values of T and therefore $\mathcal{R}_p$ is a strictly decreasing function of temperature. For the second relation of non-overlapping bands (3.15b), a similar analysis would show that $\partial \mathcal{R}_p / \partial T > 0$ and $\mathcal{R}_p$ is a strictly increasing function of temperature.

B. PARTIALLY OVERLAPPING AND COMMON BAND LIMIT CASE

In this section, the case which is partially overlapping and the common band limit case are considered. Two sets of relations are considered in this case and they are

$$1 \le x_3 < x_2 < x_4 \text{ or } 1 < x_3 < x_2 \le x_4 \tag{3.19a}$$

$$x_3 \le 1 < x_4 < x_2 \text{ or } x_3 < 1 < x_4 \le x_2 \tag{3.19b}$$

For this discussion, the graphical method previously introduced is useful [Ref. 8: pp. 1258]. Figure 4 illustrates the first set of the relations (3.19a) for partial overlap. With reference to Figure 4, six sets of integrals are defined as follows:

$$S_1 = \int_{\alpha}^{\alpha x_3} f(\psi) d\psi \quad A_1 = \int_{\alpha}^{\alpha x_3} g(\psi) d\psi \tag{3.20a,b}$$

$$S_2 = \int_{\alpha x_3}^{\alpha x_2} f(\psi) d\psi \quad A_2 = \int_{\alpha x_3}^{\alpha x_2} g(\psi) d\psi \tag{3.20c,d}$$

$$S_3 = \int_{\alpha x_2}^{\alpha x_4} f(\psi) d\psi \quad A_3 = \int_{\alpha x_2}^{\alpha x_4} g(\psi) d\psi. \tag{3.20e,f}$$

After inserting this formalism into (3.9), the bracketed operator [f,g] becomes

$$[f,g](1, x_2, x_3, x_4, \alpha) = (S_1 + S_2)(A_2 + A_3) - (A_1 + A_2)(S_2 + S_3). \qquad (3.21a)$$

After expansion and recombination of (3.21a), it follows

$$[f,g](1, x_2, x_3, x_4, \alpha) = [A_3(S_1 + S_2) - S_3(A_1 + A_2)] + (S_1A_2 - A_1S_2). \qquad (3.21b)$$

This can be retranslated using (3.20) into two terms which follow

$$[f,g](1, x_2, x_3, x_4, \alpha) = [f,g](1, x_2, x_2, x_4, \alpha) + [f,g](1, x_3, x_3, x_2, \alpha). \qquad (3.21c)$$

Case (3.19a) will now be applied on expression (3.21c). If $1 < x_3 < x_2 < x_4$, then both terms in (3.21c) are of the form $1 < x_2 = x_3 < x_4$ which satisfies the nonoverlap condition (3.15a). Since, as indicated in the previous section, the particular nonoverlap condition (3.15a) generates negative values for [f,g], the expression (3.21c) must be negative for the stated inequality.

For common band limit case, which is $1 = x_3 < x_2 < x_4$ or $1 < x_3 < x_2 = x_4$, one of the terms in (3.21c) becomes zero. However, the other term remains negative, and therefore [f,g] remains negative. This discussion implies that the ratio $\mathcal{R}_\rho$ is a strictly decreasing function of temperature. Similarly, for the second relation of this case (3.19b), the ratio $\mathcal{R}_\rho$ is a strictly increasing function of temperature.

C. TOTALLY CONTAINED SPECTRAL-BAND CASE

This section discusses case 3, where one interval is entirely contained within the other. By the use of asymptotic approximations [Ref. 8: pp. 1258], it is possible to show that the ratio $\mathcal{R}_\rho$ may have the same value for two or more temperatures. Therefore, the measurement to determine the temperature is not unique. Two examples, which are the case where α is large and the case where α is small, are discussed.

As previously discussed, the sign of $\partial\mathcal{R}_\rho/\partial T$ is determined by the sign of [f,g]. There are two sets of relations which are $1 < x_3 < x_4 < x_2$ and $x_3 < 1 < x_2 < x_4$. The first set of

relations is arbitrarily chosen for discussion since the approach is similar for the other relation. For large or small value of α asymptotic methods are useful to determine the sign of [f,g]. (The derivation using asymptotic approximation is in Appendix B.) For the large value of α (i.e., small temperature), [f,g] is approximated as

$$[f,g] \simeq \alpha^5 x_3^2 (1 - x_3) \exp[-\alpha(x_3 + 1)]. \tag{3.22}$$

Since x_3 is greater than one, [f,g] becomes negative. For small values of α (i.e., large temperature), [f,g] is approximated as:

$$[f,g] \simeq \frac{\alpha^5}{12} [(x_4^2 - x_3^2)(x_2^3 - 1) - (x_2^2 - 1)(x_4^3 - x_3^3)]. \tag{3.23}$$

Given x_3 and x_4, it is always possible to find a sufficiently large x_2 such that (3.23) is positive. Combining the two results for small α and large α, the sign of $\partial \mathcal{R}_p / \partial T$ is not fixed over α (i.e., temperature). This means that the ratio $\mathcal{R}_p$ does not have a one-to-one correspondence with temperature. Therefore, for the case when one spectral band is completely contained within the other, the temperature determination method based on the dual spectral band measurement of photon emittance is not, in general, valid.

D. RATIO CALCULATION FOR PHOTON EMITTANCE

In order to generate the output ratio calculation, the numerical method for integration known as Simpson's rule [Ref. 12: pp. 95] was used. The flow chart for this calculation is shown in Appendix C. The examples were demonstrated using the conditions in [Ref. 8: pp. 1258-1259]. One case has a band combination of [2.5 μm, 5.5 μm] and [3.9 μm, 4.1 μm] shown in Figure 5. The second case has a band combination of [10.0 μm, 14.4 μm] and [11.8 μm, 12.2 μm] shown in Figure 6. In these figures, the normalized ratio denoted as $\tilde{\mathcal{R}}_p$ was used to enhance the results. Normalization is done by

$$\tilde{\mathcal{R}}_p = \frac{\mathcal{R}_p - \mathcal{R}_{\min}}{\mathcal{R}_{\max} - \mathcal{R}_{\min}} \tag{3.24}$$

where $\mathcal{R}_{max}$ is the maximum value of $\mathcal{R}_p$ and $\mathcal{R}_{min}$ is the minimum value of $\mathcal{R}_p$ Both cases are slightly different from the results in [Ref. 8: pp 1259], but the general features are the same. One ratio value may correspond to two or more temperature values as predicted in Section C. These figures indicate that the minima of the ratio occur in different positions depending on the bands selected.

E. DISCUSSION OF COMPUTER RESULTS

Computer simulations were performed for the three cases discussed in this chapter. The first example is the nonoverlapping case and the band pair is chosen to be [3.0 μm, 4.0 μm] and [4.0 μm, 5.0 μm]. Figure 7 shows this example and it exhibits the decreasing feature as expected in Section A. The second example is the partially overlapping case and the band pair is chosen to be [3.0 μm, 4.5 μm] and [3.5 μm, 5.0 μm]. Figure 8 shows this case and the results agree with the discussion in Section B. The third example is the case of totally contained band within the other and the band pair is [3.0 μm, 5.0 μm] and [3.5 μm, 4.5 μm]. Figure 9 represents this case and the results show that one-to-one correspondence does not exist in this case. It can be seen from Figure 9 that a ratio value of 2.0 corresponds to both 460 degrees Kelvin and 1400 degrees.

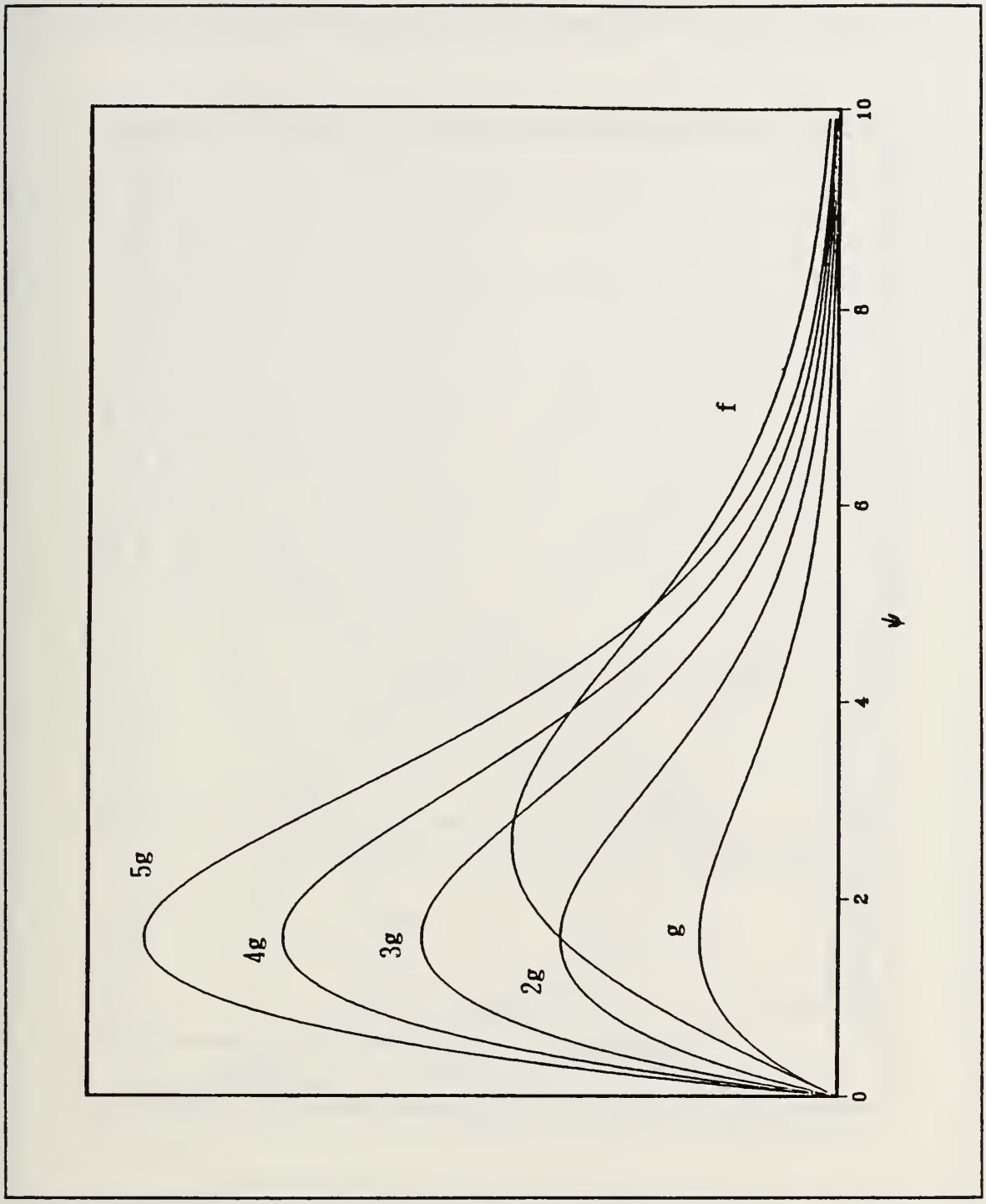

Figure 2. Plot of $f(\psi)$ and $\beta g(\psi)$ for $\beta = 1,2,...,5$

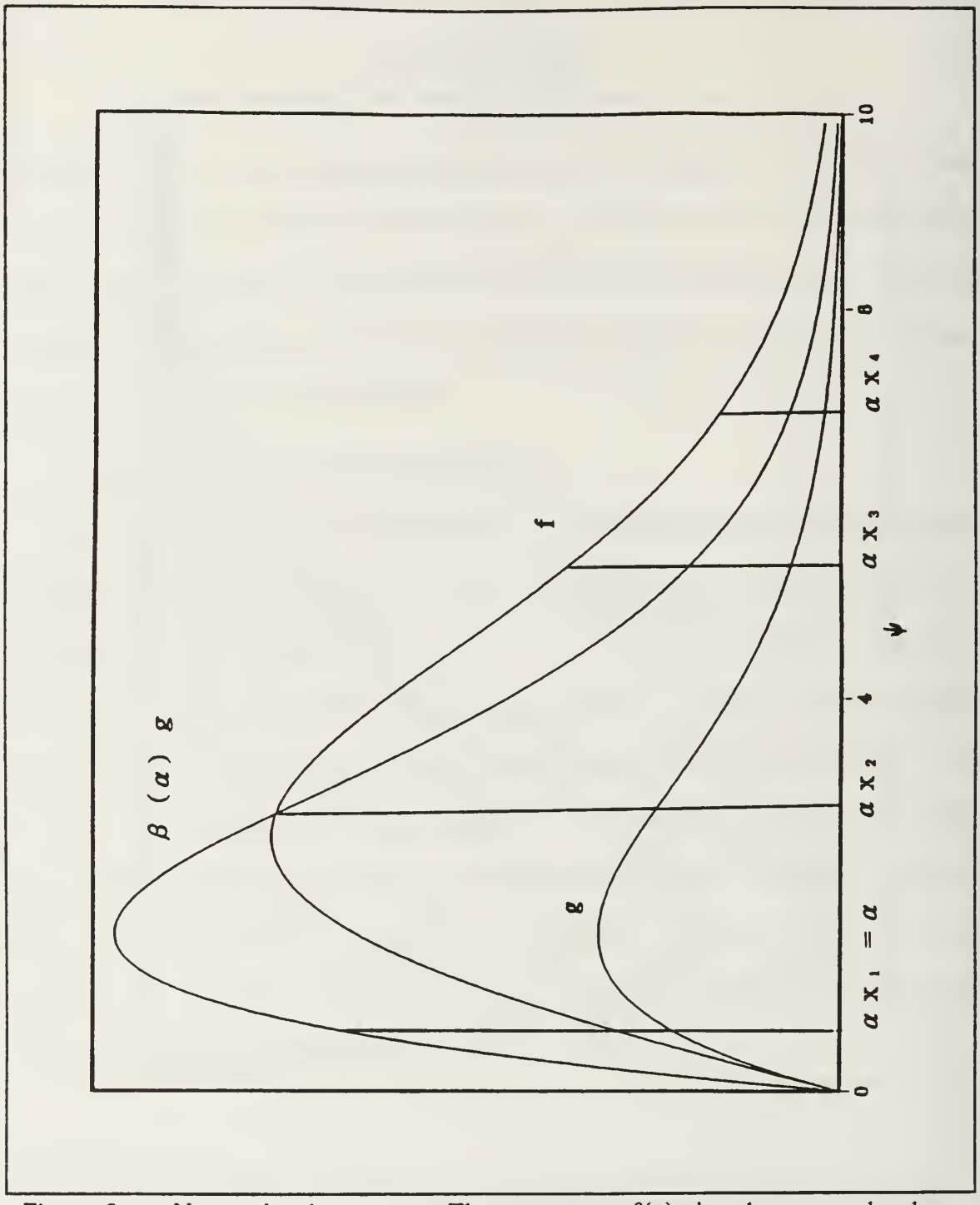

Figure 3. **Nonoverlapping case.:** The constant $\beta(\alpha)$ is chosen such that $\beta(\alpha)g(\alpha x_2) = f(\alpha x_2)$.

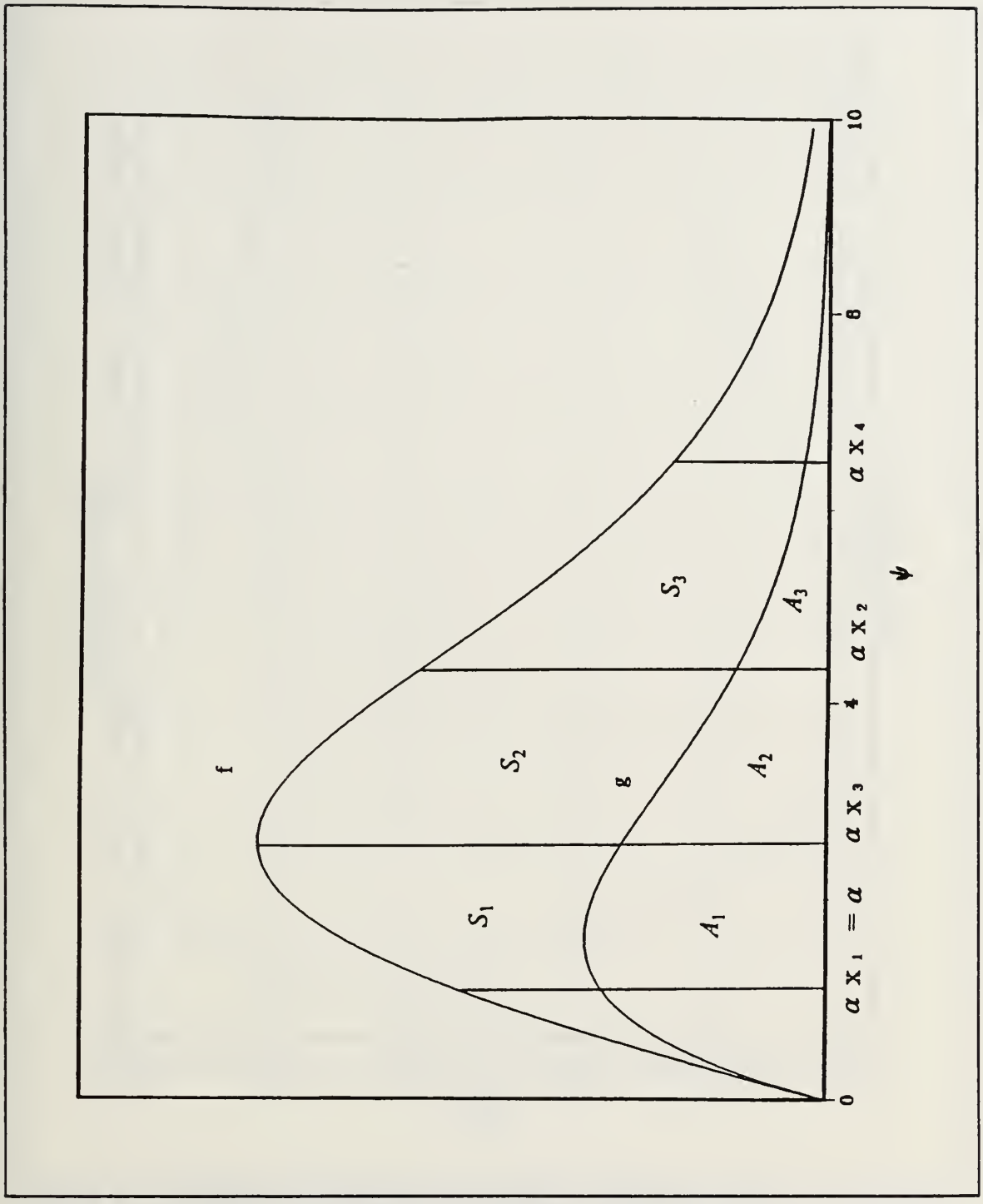

Figure 4. Partially overlapping case or common band limit case: Each region is defined in the text.

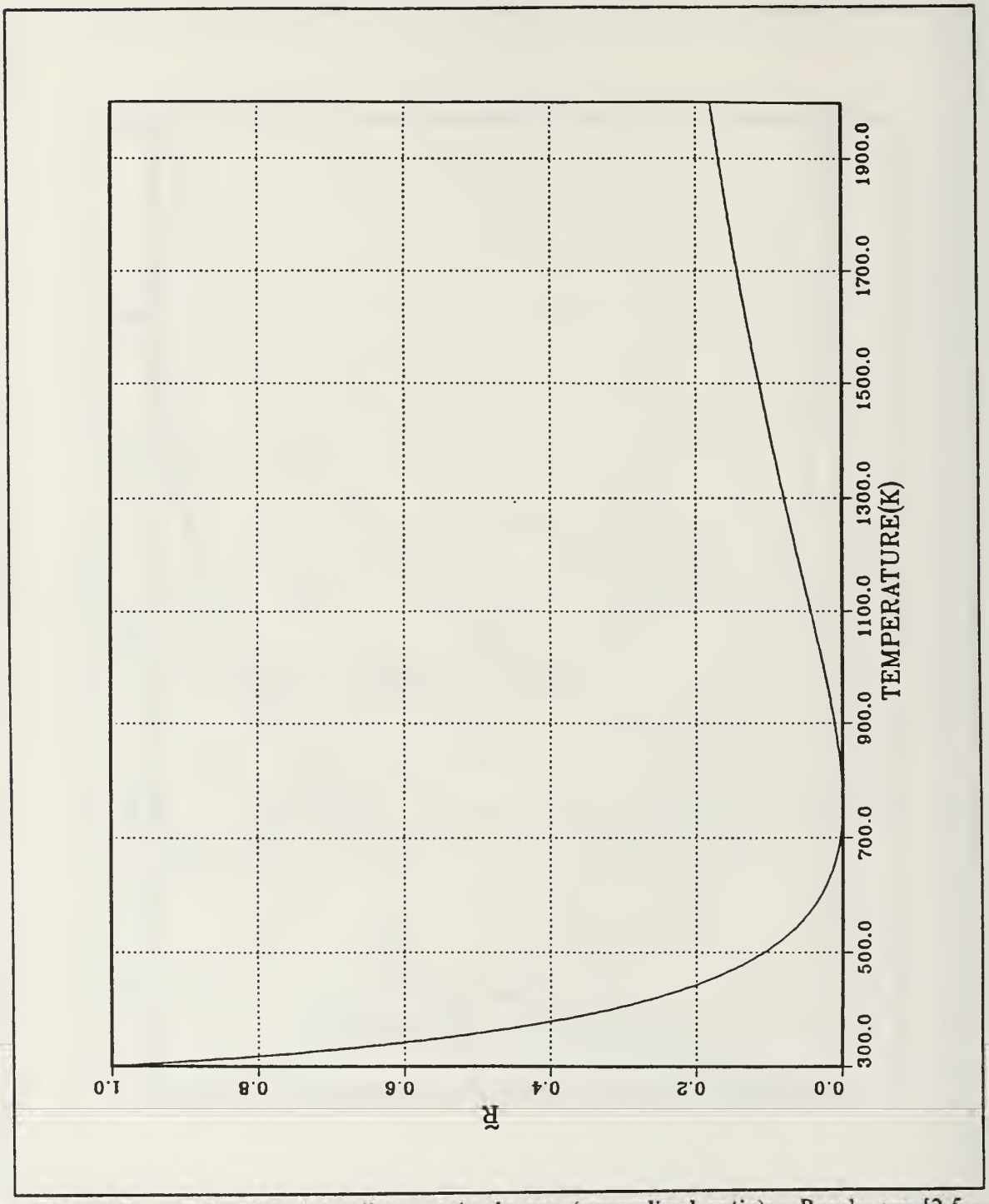

Figure 5. Example of totally contained case (normalized ratio): Bands are [2.5 μm, 5.5 μm] and [3.9 μm, 4.1 μm].

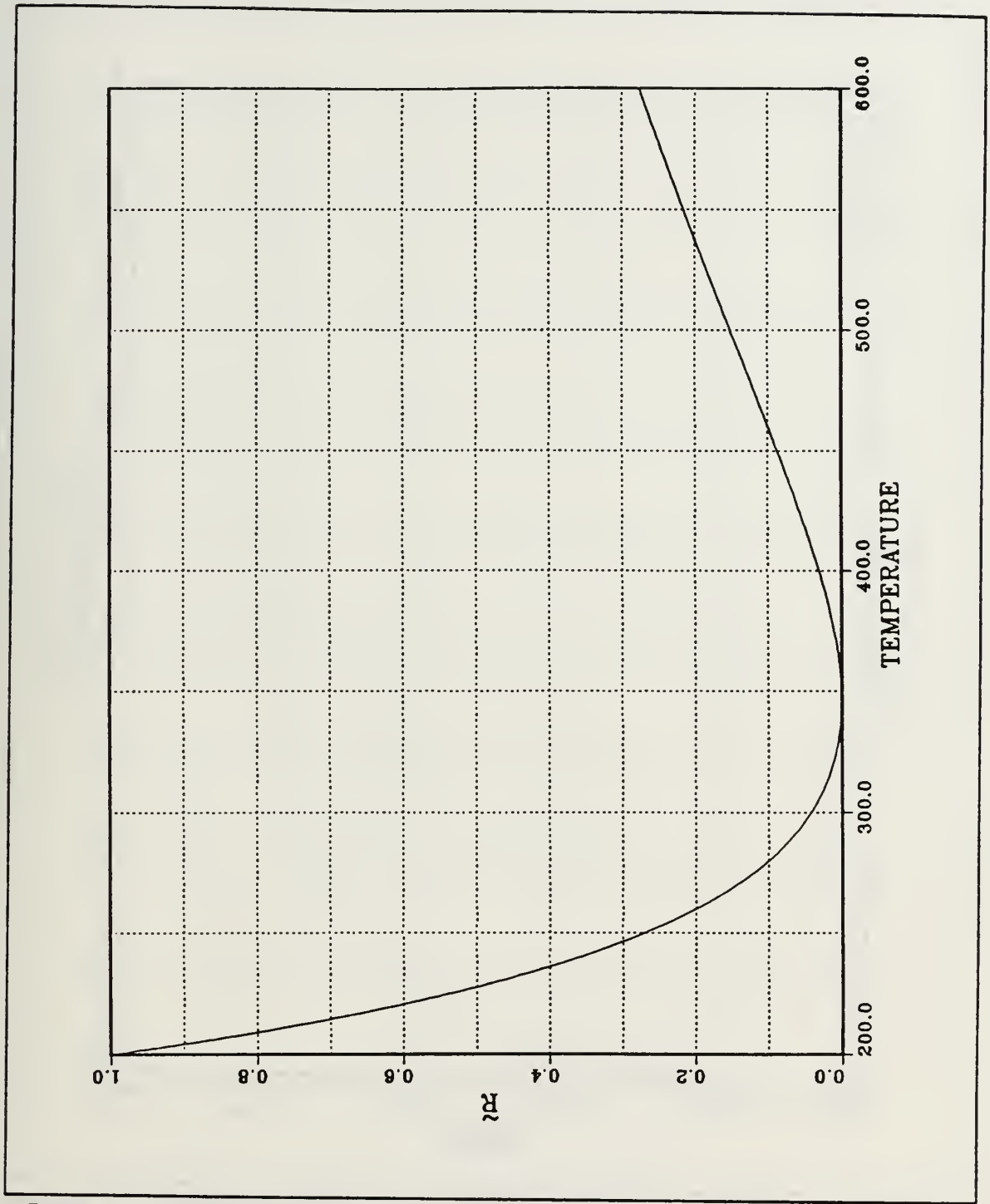

Figure 6. Example of totally contained case (normalized ratio): Bands are [10 μm, 14.4 μm] and [11.8 μm, 12.2 μm].

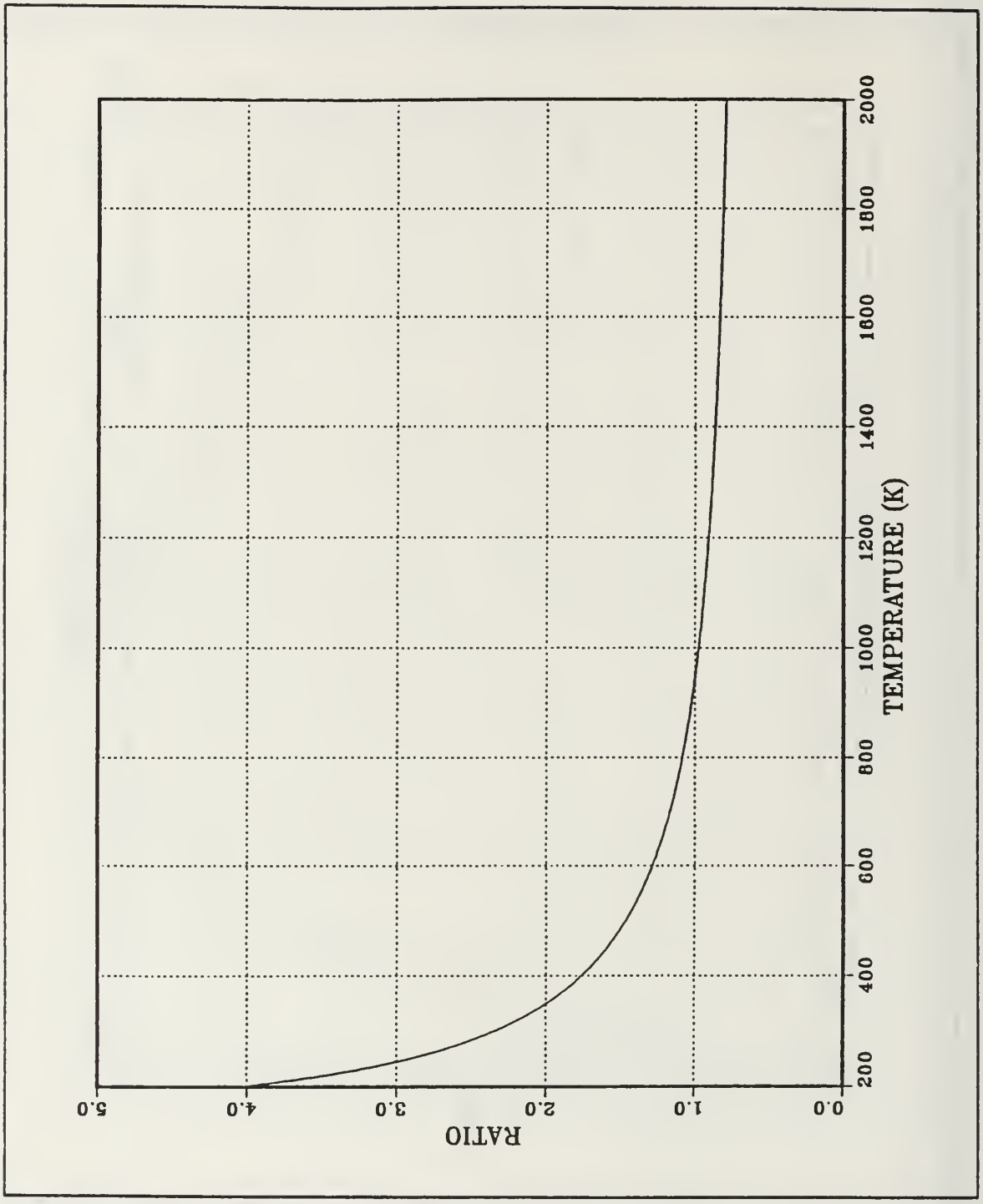

Figure 7. Example of the non-overlapping case: Bands are [4.0 μm, 5.0 μm] and [3.0 μm, 4.0 μm].

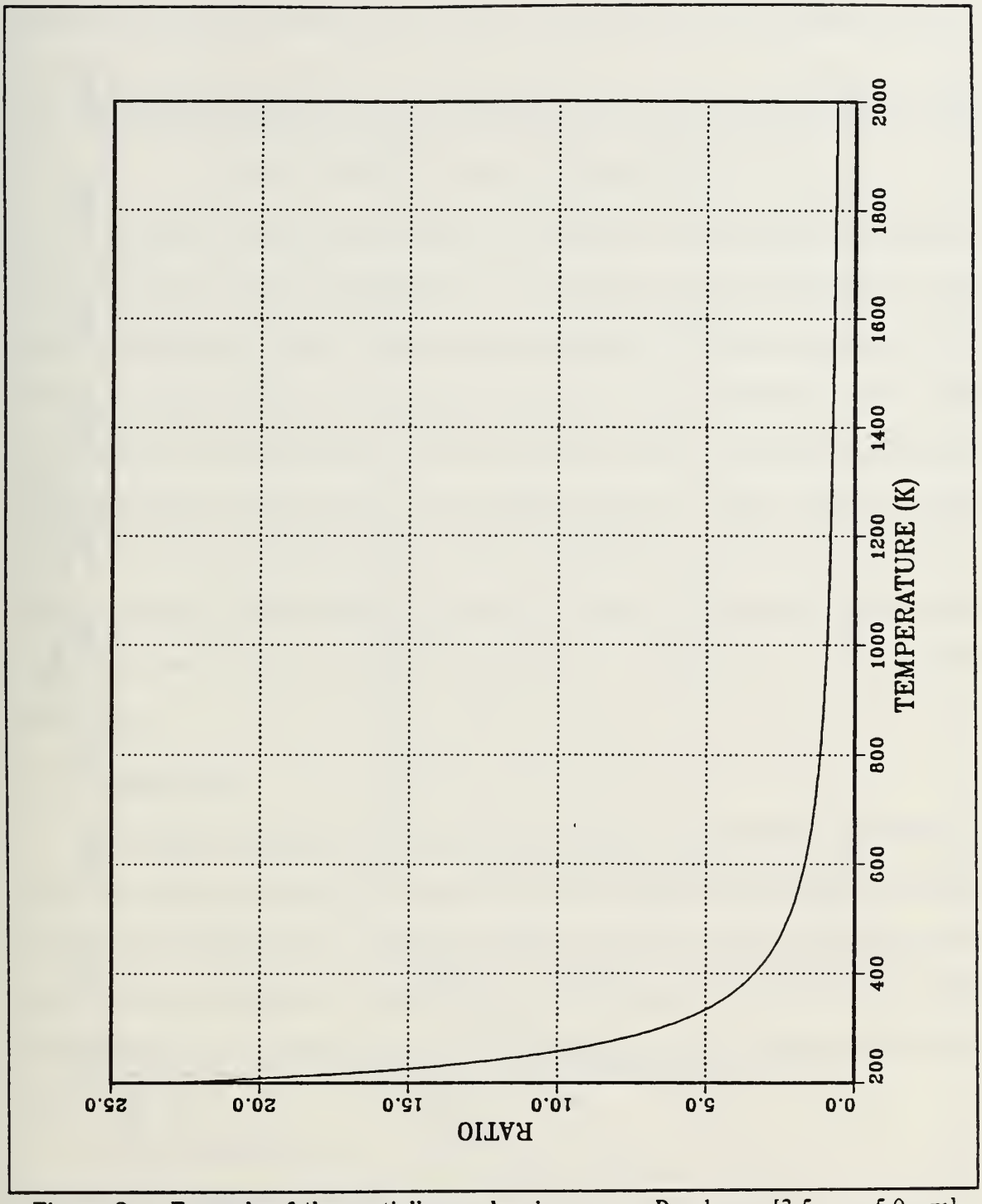

Figure 8. Example of the partially overlapping case: Bands are [3.5 μm, 5.0 μm] and [3.0 μm, 4.5 μm].

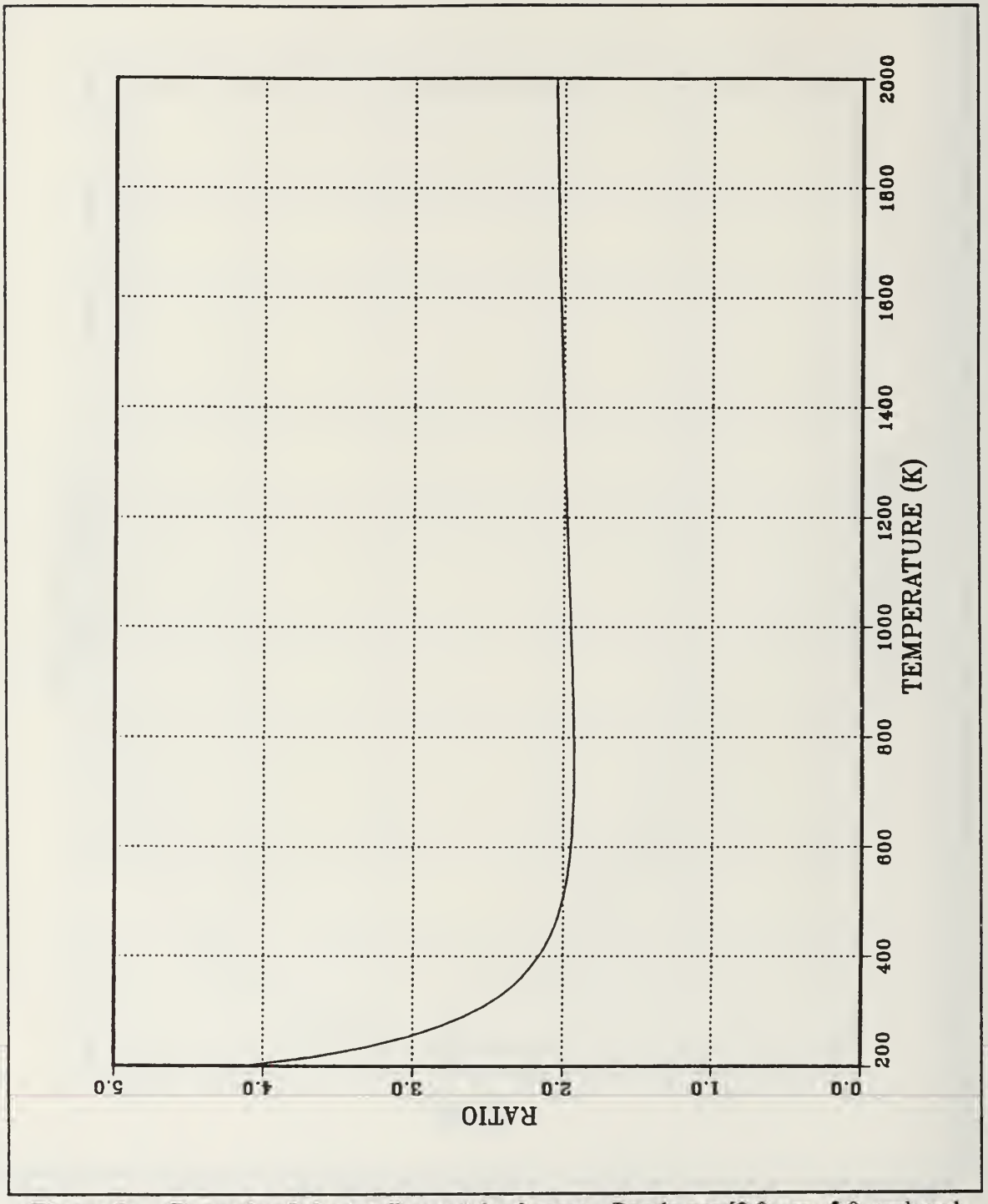

Figure 9. Example of the totally contained case: Bands are [3.0 μm, 5.0 μm] and [3.5 μm, 4.5 μm].

IV. A GENERAL MODEL FOR TEMPERATURE DETERMINATION VIA DUAL SPECTRAL BAND MEASUREMENTS

In Chapter II, ideal photon emittance temperature determination was discussed. Since this discussion was dealing with the ratio without considering measurement of the photon emittance as a system, it was not always practical. Therefore, some other factors should be taken into account to realize this method. They are emissivity of the object, atmospheric transmittance, detector responsivity, and so on. In the previous discussion, those parameters were assumed to be spectrally constant or unity. Strictly speaking, they depend on the wavelength. Also after considering these factors as part of the system, the resultant ratio becomes the ratio of the output voltages from the detectors of two bands instead of the ratio of photon emittance. A brief discussion of these parameters follow.

A. EMISSIVITY

The emissivity dictates how much thermal energy is radiated from an object. Its value lies between zero and unity depending upon the material characteristics of thermal source. It is denoted as $\varepsilon(\lambda)$. Although emissivity for some materials has temperature dependency, it is assumed to be independent of temperature to make discussion simplified. Materials are divided into three types based on the value of emissivity. They are [Ref. 3: pp. 40]

1. A black body, $\varepsilon(\lambda) = 1$.
2. A gray body, $\varepsilon(\lambda) = constant < 1$.
3. A selective absorber, $\varepsilon(\lambda)$ varies with wavelength.

The spectrally constant emissivity cases were covered in the previous Chapters II and III. Therefore, wavelength-dependent emissivity is the primary focus of discussion in this

chapter. In addition, since emissivity depends on the types of materials, it is not possible to get reliable analytical expressions for all selective absorbers. Usually emissivity values are obtained by measurement.

B. ATMOSPHERIC TRANSMITTANCE

The atmosphere is known to behave as a wavelength-selective absorber. This implies that the transmission of signals through the atmosphere becomes wavelength dependent. Specifically, the atmosphere affects the transmission of infrared radiation. The main compositions of the atmosphere are nitrogen, carbon dioxide, oxygen, and water vapor. Among these, molecules which have nonsymmetric molecular structure are primary responsible for absorption. Thus carbon dioxide and water vapor are the dominant sources for absorption. In addition some other small constituents of the atmosphere, which have non-symmetric structure, also contribute absorption.

Atmospheric scattering is the other important phenomenon which affects atmospheric transmission. The strongest atmospheric scattering occurs in the case when the size of aerosols and the wavelength of the signal are almost the same. In this particular case the scattering coefficient depends highly on a wavelength of the signal. The Mie theory describes this phenomenon.

The atmospheric transmittance is determined by atmospheric absorption coefficient and atmospheric scattering coefficient. It is given by

$$\tau(\lambda, x) = \exp\left[-(\alpha(\lambda) + \gamma(\lambda))x\right] \tag{4.1}$$

where $\alpha(\lambda)$ is atmospheric absorption coefficient, $\gamma(\lambda)$ is atmospheric scattering coefficient, and x is the distance between the object and the detector. An example transmittance data by the NPS LOWTRAN6 program [Ref. 13] at 20 meters in height, 0 degree elevation for 1 km and 5 km distances under 1962 U.S. standard atmospheric conditions are shown in Figure 10. The importance here is that the transmittance de-

pends not only the wavelength but also distance and atmospheric conditions. Moreover, atmospheric conditions vary with height and thus the transmission depends on the path between the object and the detector. Unless the path and atmospheric conditions are known, it is impossible to apply the ideal ratio calculation. Therefore, the transmission path and atmospheric conditions have to be provided in order to obtain the atmospheric transmittance. A recent report [Ref. 11: pp. 41] on transmittance calculation for the atmosphere has concluded that refraction effects can essentially be ignored.

C. DETECTOR RESPONSIVITY

The detector responsivity is generally obtained by dividing the measured output signal voltage by the optical power falling on the detector. And it is defined as

$$R \equiv \frac{V_{rms}}{HA_d} \tag{4.2}$$

where R is the responsivity [V/W], V_{rms} is the RMS output voltage, H is the RMS irradiance [W/cm^2] at the detector location, and A_d is the detector area [cm^2]. However, this quantity is not the appropriate parameter for the development of the photon emittance case. A new proposed responsivity R′ is defined by modifying (4.2) in order to adjust it for the photon emittance calculation. It is given by dividing the measured output voltage signal by the number of photons into the detector. The proposed R′ is defined as

$$R' \equiv \frac{V_{rms}}{QA_d} \tag{4.3}$$

where R′ is the photon responsivity [$V \cdot photons^{-1} \cdot s$], and Q is the photon emittance [$photons \cdot s^{-1} \cdot cm^{-2}$]. It follows from definitions (4.2) and (4.3) that the photon responsivity R′ is simply obtained by multiplying responsivity R by hc/λ,

$$R' = R\frac{hc}{\lambda}. \tag{4.4}$$

as shown above. For photon detectors sensitive to the number of photons, R′ should be fairly constant out to the cut off wavelength.

Unfortunately, detector responsivity (4.2) is not usually provided among detector specifications, but the specific detectivity D* is given instead. The D* is the normalized quantity of detectivity defined by [Ref. 3: pp. 270]:

$$D^* = D\sqrt{A_d B} \tag{4.5a}$$

where B is the electrical system bandwidth in heltz, A_d is the area of the detector, and D is the detector detectivity. This quantity is often expressed in terms of the reciprocal of the noise equivalent power (NEP). Therefore, the D* is also given by [Ref. 3: pp. 270]

$$D^* = \frac{\sqrt{A_d B}}{NEP}. \tag{4.5b}$$

The noise equivalent power is the radiant flux required to obtain an output signal equal to the noise of the detector. It is given by

$$NEP = \frac{HA_d}{\frac{V_s}{V_N}} \tag{4.6}$$

where V_s is RMS signal voltage and V_N is RMS noise voltage. From (4.6), the specific detectivity becomes

$$D^* = \frac{\frac{V_s}{V_N}\sqrt{A_d B}}{HA_d}. \tag{4.7}$$

The photon responsivity is obtained by combining (4.3), (4.4), and (4.7), and it is

$$R' = \frac{D^* V_N}{\sqrt{A_d B}} \frac{hc}{\lambda} . \tag{4.8}$$

This equation shows the specific detectivity is closely related to the photon responsivity. From the expected wavelength dependencies in (4.8), it follows that the quantity D* should increase linearly with wavelength out to the cutoff wavelength [Ref. 3: pp. 294]. Since photon detectors respond to the number of photons absorbed in the detector up to cutoff wavelength (usually dictated by the band-gap), the modified responsivity of photon detectors is ideally independent of wavelength.

D. COMPUTER SIMULATION OF TEMPERATURE DETERMINATION

Based on above discussion, the ratio of photon emittance for black body is replaced by the ratio of the output voltages at the detectors, and it is given by

$$\mathcal{R}_p^M = \frac{\int_{\alpha}^{\alpha x_2} \varepsilon(\lambda)\tau(\lambda, x)R'_1(\lambda)g(\psi)d\psi}{\int_{\alpha x_3}^{\alpha x_4} \varepsilon(\lambda)\tau(\lambda, x)R'_2(\lambda)g(\psi)d\psi} \tag{4.9}$$

where $\varepsilon(\lambda)$ is the emissivity, $\tau(\lambda, x)$ is atmospheric transmittance, and $R'(\lambda)$ is the photon detector responsivity. The subscript on the photon detector responsivity denotes the spectral band used in the measurement. In this equation, assuming that the wavelength parameters are spectrally constant and two identical detectors are used, the ratio becomes identical to the ratio of photon emittance for black body (3.6). In order to generate the output ratio calculation under more general conditions, the numerical method for integration known as Simpson's rule [Ref. 12: pp. 95] is used. The algorithm for this calculation is shown in Appendix D.

1. Discussion of the computer simulations

As described in this chapter, the actual ratio for the photon detector is the ratio of the output voltages. In the rest of this section, the simulation for the ratio calculation is discussed. Although the photon detector responsivity has wavelength dependence, as discussed in Section C, it is not a very sensitive factor up to the detector cut-off. Therefore, this is ignored in this discussion, and emissivity and atmospheric transmittance are considered. Since emissivity depends on the material of the thermal source, many kinds of emissivity values are possible. For this simulation, an arbitrary created emissivity curve shown in Figure 11 was used. For atmospheric transmittance, the atmospheric conditions of 1962 U.S. standard atmosphere were selected. The data, shown in Figure 10, are obtained from NPS LOWTRAN6 program. For the purpose of comparison with the results for ideal case, the same band pairs are selected as ones in Chapter III. The result for overlapping case is shown in Figure 12, for partially overlapping case in Figure 13, and totally contained case in Figure 14. The curves generated in these figures correspond to 1 km and 5 km. With the exception of Figure 14, there is a one-to-one correspondence between measured ratio and temperature for each range. In Figure 14, there is a slight positive shape after $T = 1300$ K which violates the uniqueness condition. Although the values are shifted slightly, the shapes of the curves are essentially the same as ones for ideal ratio case shown in Chapter III. The general features of each case are the same. However, the results demonstrate that the curves depend on distance. This is quite inconvenient. The application of two-band temperature determination is then impossible without range information. Also, to lesser extent, the application is limited since the emissivity is material dependent. If the source for thermal radiation is not a gray body, then the emissivity of the source needs to be known in advance.

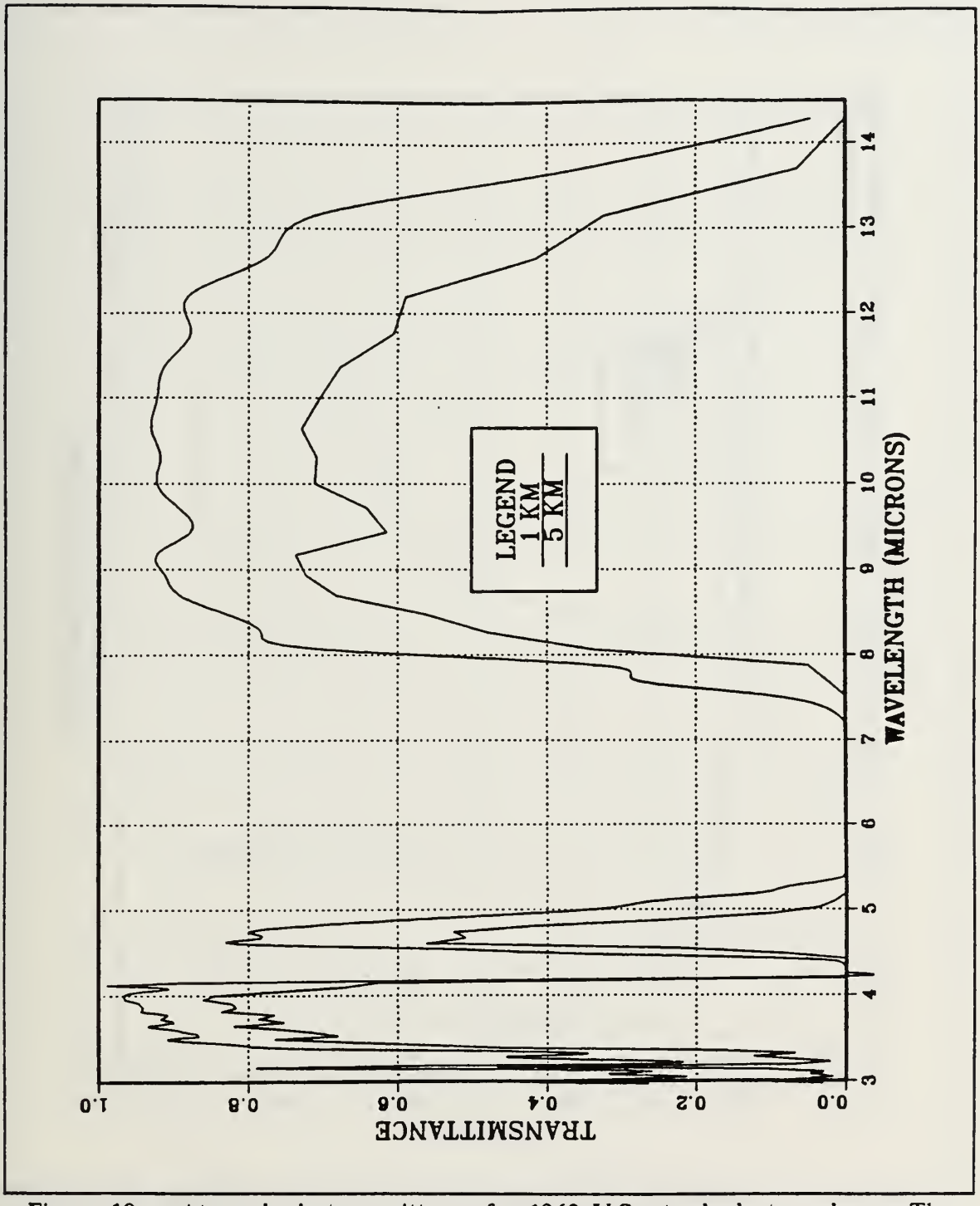

Figure 10. Atmospheric transmittance for 1962 U.S. standard atmosphere: The path lengths are taken to be 1 km and 5 km in the horizontal direction.

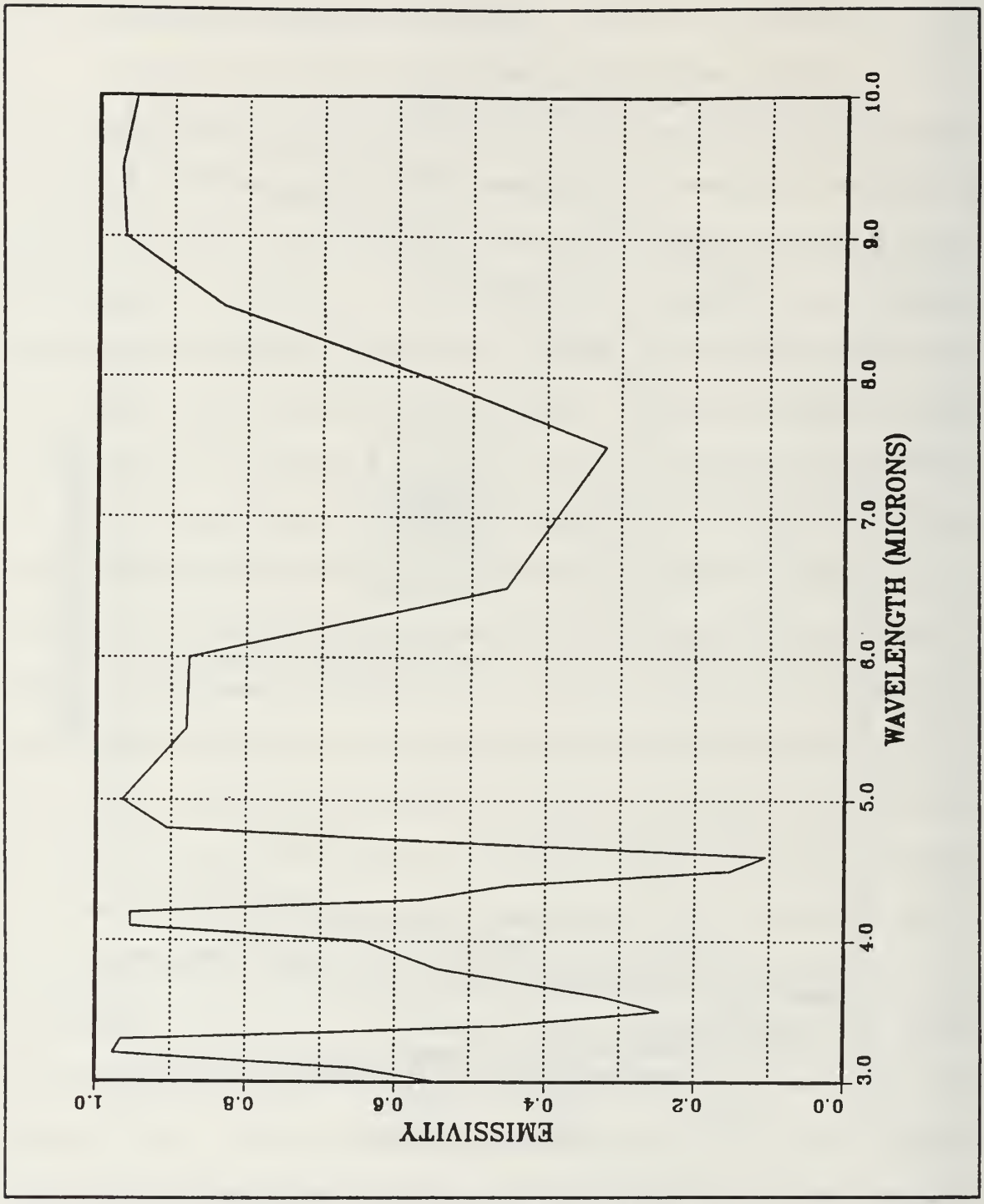

Figure 11. Example of the emissivity (arbitrary chosen): This data does not correspond to the specific material.

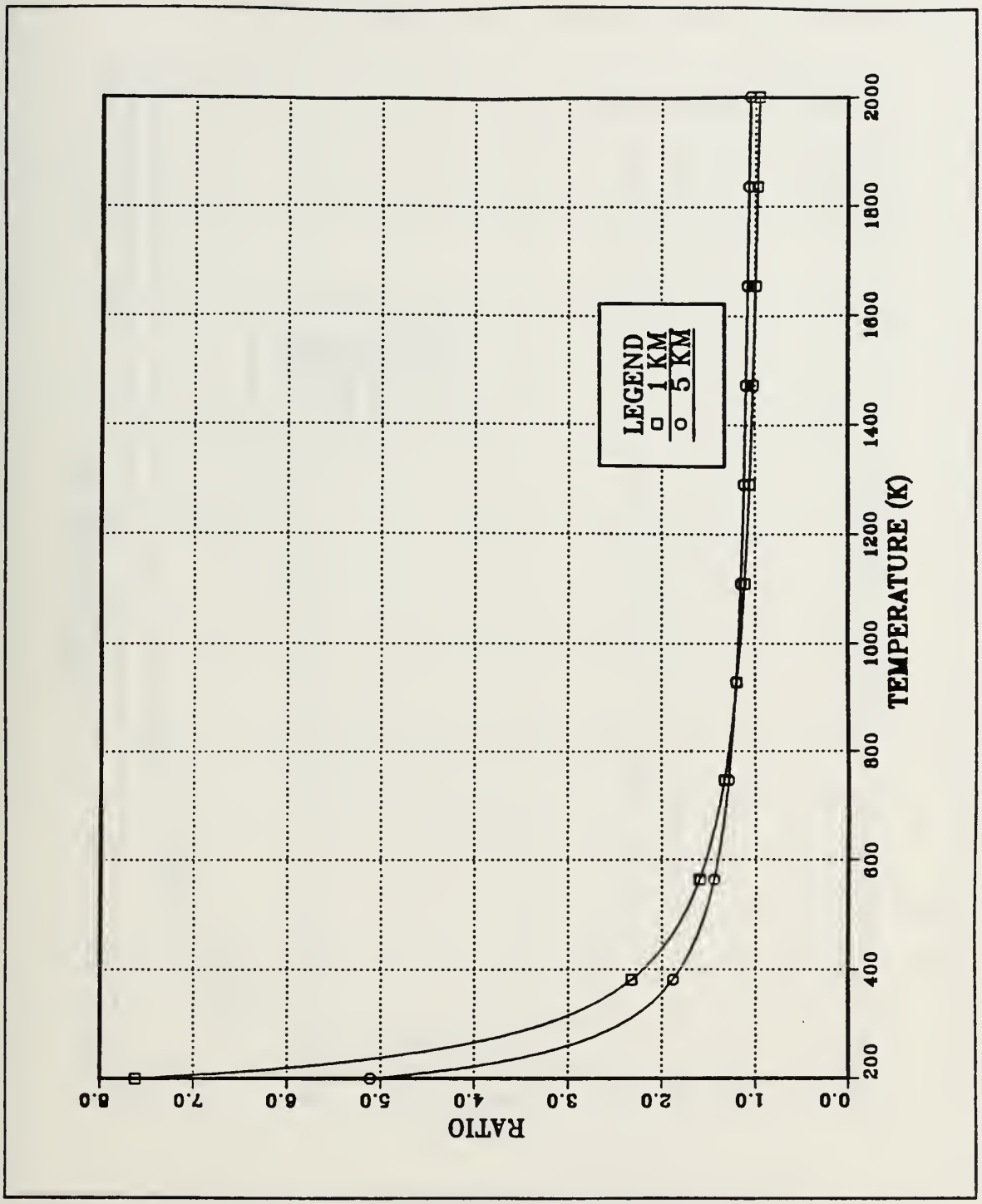

Figure 12. **The ratio of output voltages for nonoverlapping case:** Bands are (5.0 μm, 4.0 μm) and (4.0 μm, 3.0 μm). The distances are 1 km and 5 km.

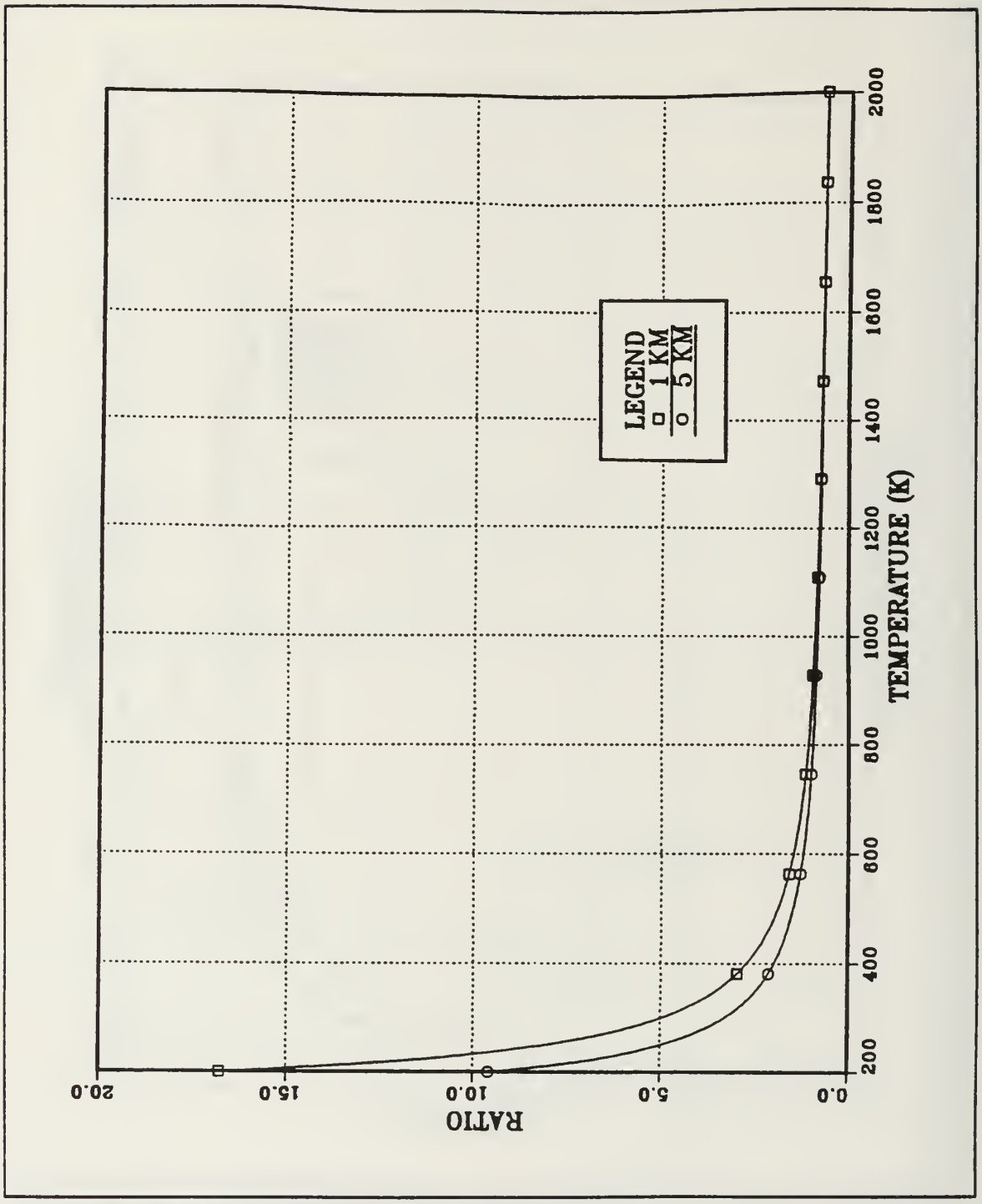

Figure 13. The ratio of output voltages for partially overlapping case: Bands are (5.0 μm, 3.5 μm) and (4.5 μm, 3.0 μm). The distances are 1 km and 5 km.

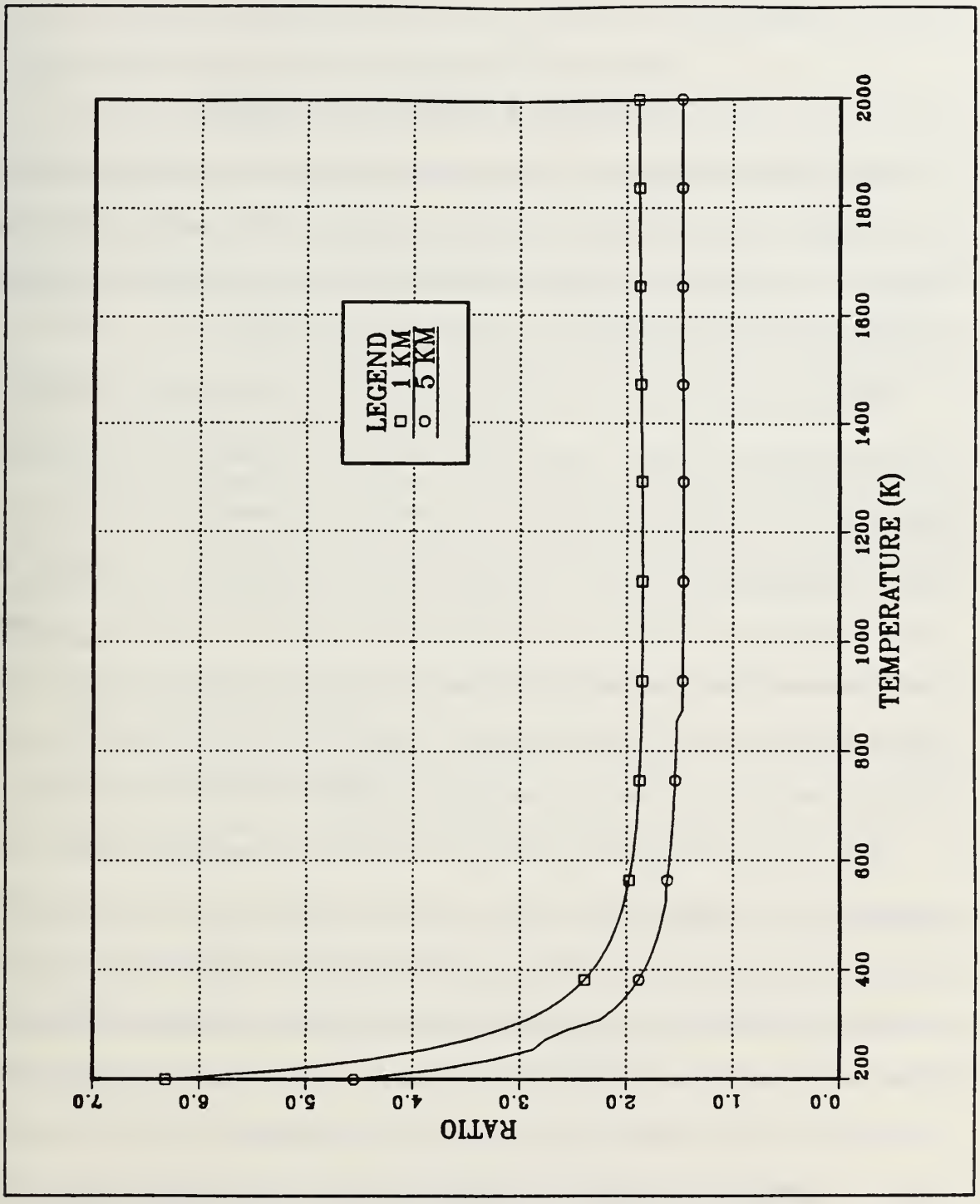

Figure 14. The ratio of output voltages for totally contained band case: Bands are (5.0 μm, 3.0 μm) and (4.5 μm, 3.5 μm). The distances are 1 km and 5 km.

V. THERMAL RANGING TECHNIQUE

From the previous chapter, the ratio of output voltages from dual spectral bands is not the same as the ratio of black body photon emittances under realistic and nonideal conditions. To solve and apply the method under these conditions can be quite difficult. On the other hand, one significant idea is hidden in this problem.

The concept presented in this chapter is created from the difficulty, in the temperature determination method, produced by nonconstant atmospheric transmittance. Among assumptions discussed in Chapter IV, atmospheric transmittance breaks the validity of temperature determination procedure because it depends on wavelength, the distance between an object and the detector, and atmospheric conditions. Although emissisivity and detector responsivity have to be taken into account, under some reasonable assumptions they can be neglected. It will be shown that the dependency of atmospheric attenuation on the distance makes the concept of thermal ranging feasible.

The use of infrared thermal signals has the advantage that active interrogation is not required since the object radiates energy or photons. This passive property of infrared detection can be significantly important in military situations. However, the passive detection of the target does not automatically provide range data and this is a disadvantage of thermal infrared detection systems. One interactive (nonautomatic) passive system involves the use of a trained human observer. The training allows the observer to recognize a target and by noting the size of the target on the screen make an experienced estimate of the range. Currently ranging is done by active sensor systems such as radar or laser range finder. These active systems are capable of being sensed by the target. Although active ranging systems tend to provides precise distance information, they ex-

pose the instrument generating the signal. Therefore, the development of a passive ranging system would provide significant military advantage.

The Electronic Support Measure (ESM) equipment in electronic warfare systems is the passive sensor in the microwave region. This gives target identification, direction of the target and also a very rough range information. For this method, the power transmitted by a radar of a target, the antenna gain, and attenuation factor must be obtained in advance. It seems that the same concept can be applied to infrared systems only if the temperature of a target, surface area, emissivity, and atmospheric transmittance are known. Therefore, this method is not practical.

The following discussion proposes a new concept of passive ranging by infrared systems. It will be shown that this concept is a feasible solution to the problem of target ranging using only automatic passive methods. The following discussion consists of three steps:

1. Step 1: Atmospheric attenuation coefficient is assumed to be constant. Temperature of the target is known.
2. Step 2: Atmospheric attenuation coefficient is assumed to be constant. Temperature of the target is unknown.
3. Step 3: Atmospheric attenuation coefficient is not constant. Temperature of the target is unknown.

The concept of ranging shown here is based on the distance dependency of atmospheric transmittance. Step 1 and step 2 are intermediate procedures and they do not allow changing atmospheric conditions due to, for example, an elevated transmission path. In step 3, these prohibitions are rescinded and the ranging model has greater applicability.

A. RANGING FOR KNOWN TEMPERATURE CONDITION WITH HOMOGENEOUS ATMOSPHERIC CONDITIONS

In the analysis of this section the emissivity of the target and photon detector responsivity are assumed to be spectrally constant. In addition, it is assumed that at-

mospheric conditions are not changing along a line-of-sight trajectory between target and passive sensor system. Therefore, atmospheric attenuation coefficients will not depend on range but still exhibit wavelength dependence. By appropriate band selection, i.e., from a flat portion of the transmission curve [LOWTRAN], the wavelength dependence of the transmission can be approximately neglected with in each of the selected bands. Therefore, atmospheric transmittance for the i-th band is given by

$$\tau_i(x) = \exp(-\sigma_i x) \tag{5.1}$$

where σ_i is the atmospheric attenuation coefficient within the i-th band, and x is the transmission path length. Applying the assumptions stated to the ratio (4.9) leads to

$$\mathscr{R}^M = \frac{\tau_1(x)}{\tau_2(x)} \mathscr{R}^I. \tag{5.2a}$$

After substitution of (5.1), the ratio can be written as

$$\mathscr{R}^M = \exp[-(\sigma_1 - \sigma_2)x]\mathscr{R}^I \tag{5.2b}$$

where $\mathscr{R}^M$ is the ratio of the measured output voltage at the detector, $\mathscr{R}^I$ is the ideal ratio of photon emittance, and σ_i are the atmospheric attenuation coefficient for the measured bands. In (5.2b), the ratio of the output voltages is obtained by direct measurement. The atmospheric attenuation coefficient is calculated from the atmospheric conditions, and the ratio of photon emittance is determined by the temperature given. Therefore, the transmission path length is the only unknown parameter. From (5.2b), the transmission path distance is obtained as

$$x = -\frac{1}{\sigma_1 - \sigma_2} \ln \frac{\mathscr{R}^M}{\mathscr{R}^I}. \tag{5.3}$$

The use of (5.3) makes passive thermal ranging feasible. However, it is applicable to very limited conditions. In the battle field, the targets are usually unknown, and consequently the temperature of the target is hard to obtain. This means that the system should be capable of determining both range and temperature to be practical. The new proposed concept is described in the following sections.

B. RANGING FOR UNKNOWN TEMPERATURE WITH HOMOGENEOUS ATMOSPHERIC CONDITIONS

In this section a concept to determine the range and the temperature of the target is discussed. As in Section A, the atmospheric conditions are assumed to be homogeneous in space. Mathematically, two nondegenerate equations can be used to solve for two unknowns. In this discussion, the two unknowns are range and temperature of a target. To get two equations, two distinct sets of ratio calculations are required. For that purpose, no less than three sets of band measurements (i.e., band 1, band 2, and band 3) are required to produce two distinct equations such as (5.3). All the assumptions described in the previous section are also applied in this section except that the temperature of a target is unknown. The mathematical derivation to get the range equations is exactly the same as in the previous section. The two range equations for three sets of band measurements are

$$x = -\frac{1}{\sigma_1 - \sigma_2} \ln \frac{\mathscr{R}_{12}^M}{\mathscr{R}_{12}^I} \tag{5.4}$$

$$x = -\frac{1}{\sigma_2 - \sigma_3} \ln \frac{\mathscr{R}_{23}^M}{\mathscr{R}_{23}^I} \tag{5.5}$$

where the subscripts serve as an index to identify spectral bands. Combining (5.4) and (5.5), one equation to solve the temperature is obtained as

$$\frac{1}{\sigma_1 - \sigma_2} \ln \frac{\mathcal{R}_{12}^M}{\mathcal{R}_{12}^I} = \frac{1}{\sigma_2 - \sigma_3} \ln \frac{\mathcal{R}_{23}^M}{\mathcal{R}_{23}^I} \tag{5.6}$$

However, this equation is impossible to solve analytically. A numerical method can be used to solve this equation. After getting the temperature, the range is easily obtained by using (5.4) or (5.5). Since the assumption that the atmospheric conditions are homogeneous in space is only approximately valid for very short ranges, this method is not practical. The following section solves the difficulty of the determination of the range without assuming homogeneous atmospheric conditions.

C. RANGING FOR UNKNOWN TEMPERATURE WITH INHOMOGENEOUS ATMOSPHERIC CONDITIONS

For the following discussion, several equations are recalled for convenience. For four bands, the ideal ratios calculated from photon emittance are defined as:

$$\mathcal{R}_{12}^I = \frac{Q(\lambda_1, \lambda_2, T)}{Q(\lambda_3, \lambda_4, T)}, \tag{5.7a}$$

and

$$\mathcal{R}_{34}^I = \frac{Q(\lambda_5, \lambda_6, T)}{Q(\lambda_7, \lambda_8, T)}, \tag{5.7b}$$

where the total photon emittance is given by

$$Q(\lambda_i, \lambda_j, T) = \int_{\lambda_j}^{\lambda_i} Q_\lambda(\lambda, T) d\lambda, \tag{5.8}$$

and spectral photon emittance Q_λ can be expressed in terms of the gray body distribution

$$Q_\lambda = \frac{2\pi\varepsilon c}{\lambda^4[\exp(hc/kT) - 1]}. \tag{5.9}$$

With two band measurements, the temperature can be determined. With three band measurements, it should be possible to determine both temperature and range. As previously discussed, range information is available as long as the effective atmospheric attenuations in each band are distinct. The problem posed by obtaining range information for a thermal source at the same elevation as the receiver (homogeneous atmospheric conditions) is not as complex as that associated with arbitrary elevation. Elevation changes in the trajectory of the radiation usually require consideration due to the curvature of the earth. In the general problem to be solved, both the receiver and the thermal source take arbitrary locations in the plane defined by the vertical line passing through the receiver and thermal source. This is represented in Figure 15.

In the algorithm to be discussed, three arbitrary but distinct radiation bands are selected. Initially disregarding the effects due to the atmospheric attenuation, calculated ideal ratios of signals are given by

$$\mathcal{R}^I_{12}(T) = \frac{\text{Ideal signal Band 1}}{\text{Ideal signal Band 2}}. \tag{5.10a}$$

$$\mathcal{R}^I_{31}(T) = \frac{\text{Ideal signal Band 3}}{\text{Ideal signal Band 1}}. \tag{5.10b}$$

Figure 16 shows the temperature dependence of these curves for bands defined by:

$$(\lambda_1, \lambda_2) = (12.0\ \mu m, 10.8\ \mu m)$$

$$(\lambda_3, \lambda_4) = (10.8\ \mu m, 9.6\ \mu m)$$

$$(\lambda_5, \lambda_6) = (9.6\ \mu m, 8.2\ \mu m)$$

The atmospheric attenuation in the form of transmittance is provided from the NPS LOWTRAN6 program [Ref. 13] using data corresponding to a vertical path. Attenuation coefficients are derived from

$$\sigma_{ij}(\lambda) = -\frac{1}{r_j} \ln \tau_{ij}(\lambda) \quad [nepers/m] \tag{5.11}$$

where i= 1,2,3 indicate the wavelength band and j is the index of the specific layer. The quantity r_j is the length of the trajectory in the j-th atmospheric layer. See Figure 17. Each r_j has the same length if the line-of-sight angle is 90 degree. The attenuation coefficient σ_{ij} is obtained by taking the 90 degree angle. The standard band average for τ_{ij} is given by

$$\tau_{ij} = \frac{\int_{\lambda_{lower}}^{\lambda_{upper}} \tau_{ij}(\lambda) d\lambda}{\Delta\lambda}. \tag{5.12}$$

With reference to Figure 18, the effective approximate transmission factor τ_i, for the i-th band, is given by:

$$\tau_l = \exp\left(-\sum_{k=1}^{k_{max}} \sigma_{l(k+m-1)} r_k\right) \tag{5.13}$$

where k_{max} is the number of layers between source and receiver, and m is the layer number of the receiver. Here, r_k is the length of the trajectory in the layer $k + m - 1$. The approximation involved in (5.12) will be discussed at the end of this section. Expression (5.13) can be recast into the form:

$$\tau_i = \exp(-\sigma_i R) \tag{5.14}$$

where

$$\sigma_i = \frac{\sum_{k=1}^{k_{max}} \sigma_{i(k+m-1)} r_k}{R} \tag{5.15}$$

and when the range R must satisfy:

$$R = \sum_{k=1}^{k_{max}} r_k. \tag{5.16}$$

With the exception of the first and final layer, the value for each r_i is obtained from the rule

$$r_i = R_i - \sum_{j=1}^{i-1} r_j \tag{5.17}$$

as shown in Figure 19. Each R_i is calculated from the Cosine Law relation derived from the geometry of Figure 20

$$(H_i + R_E)^2 = R_i^2 + (h_d + R_E)^2 - 2R_i(h_d + R_E)\cos(\theta + \frac{\pi}{2}) \tag{5.18a}$$

or equivalently

$$(H_i + R_E)^2 = R_i^2 + (h_d + R_E)^2 + 2R_i(h_d + R_E)\sin\theta, \tag{5.18b}$$

where θ is the line of sight angle between receiver and source measured with respect to the horizontal. R_l can be obtained from (5.18) using the quadratic formula with the correctly chosen '+' sign. R_1 is also obtained from (5.18) after taking

$$H_1 = [int(\frac{h_d}{\Delta r}) + 1]\Delta r \tag{5.19}$$

where the int[_] results in the integer part. This follows from examination of the geometry in Figure 15. For $R_2,...,R_k$, R_k values for H_k follow

$$H_k = H_1 + (k-1)\Delta r \tag{5.20}$$

which are used in (5.18) to calculate subsequent R_k. For clarity, it is noted that:

$$R_1 = r_1 \tag{5.21a}$$

$$R_k = r_1 + r_2 + ... + r_k \tag{5.21b}$$

until $k = k_{max}$ as defined by (5.16). Equations (5.17) combined with (5.20) are solved iteratively to generate the values for r_i except for r_{fin}. Lastly, r_{finol} is calculated from:

$$r_{k_{max}} = r_{final} = R_{k_{max}} - R_{k_{max}-1}. \tag{5.22}$$

Once r_i are determined for all i up to k_{max}, the effective transmission for each band (5.14) can be calculated from (5.15) and (5.16). The measured ratios, i.e., including the effects of the atmosphere, are related to ideal ratios (5.7) according to:

$$\mathcal{R}_{12}^{M} = \mathcal{R}_{12}^{I} \frac{\tau_1}{\tau_2} \tag{5.23a}$$

and

$$\mathcal{R}_{31}^{M} = \mathcal{R}_{31}^{I} \frac{\tau_3}{\tau_1}, \tag{5.23b}$$

in agreement with (5.2a). After substitution from (5.14), (5.23) can be written as

$$\mathcal{R}_{12}^{M} = \mathcal{R}_{12}^{I} \exp\left[-(\sigma_1 - \sigma_2)R\right] \tag{5.24a}$$

and

$$\mathcal{R}_{31}^{M} = \mathcal{R}_{31}^{I} \exp\left[-(\sigma_3 - \sigma_1)R\right], \tag{5.24b}$$

where R is the distance between thermal source and receiver. Figure 21 shows the measured ratios calculated from (5.24) for conditions:

- $\sigma_1 = 0.0001494$ [*nepers/m*]
- $\sigma_2 = 0.0001027$ [*nepers/m*]
- $\sigma_3 = 0.0004622$ [*nepers/m*]
- $R = 100$ [*m*]

Solving for R from (5.24), it follows that

$$R^{12}(T) = \frac{1}{\sigma_1 - \sigma_2} \ln \frac{\mathcal{R}_{12}^{M}}{\mathcal{R}_{12}^{I}(T)}, \tag{5.25a}$$

and

$$R^{31}(T) = \frac{1}{\sigma_3 - \sigma_1} \ln \frac{\mathcal{R}_{31}^{M}}{\mathcal{R}_{31}^{I}(T)}, \tag{5.25b}$$

where the subscripts are employed to denote spectral bands. In the algorithm, it will be assumed that the correct measured ratios, consistent with (5.24), are provided by experimental testing. Ideal ratio curves can always be calculated according to the methods (5.10) previously discussed. Constants σ_1, σ_2, σ_3 can be approximately calculated from the

NPS LOWTRAN6 data. By checking for the crossing point between the two curves (5.25), both the temperature, T, and the range, R, are uniquely determined as shown in Figure 22.

The algorithm sketched out is not yet complete. The values of σ_1, σ_2, and σ_3 are dependent on the range, R, since the weights for evaluating the coefficients σ_i (5.15) depend on all the values for r_i. In order to calculate the coefficients σ_i (5.15), an initial guess is made for a range candidate, R_{G0}, within limits dictated by the domain of LOWTRAN data sampled. This value for R_{G0} is used in the calculation of σ_1, σ_2, and σ_3. The search for a numerical crossing point for curves (5.25) produces a new value for R which can be denoted as R_{G1}. The value for R_{G1} generated by this first iteration is expected to be closer to the actual range but with an unacceptable level of error. The process is repeated by iterating with the R_{G1}. The next estimate generated by the algorithm, R_{G2}, is tested against the previous one, R_{G1}. In general, the procedure is stopped when

$$\left| \frac{R_{Gm} - R_{Gm-1}}{R_{Gm}} \right| < \delta. \tag{5.26}$$

where δ is the predetermined convergence parameter and the index m specifies the number of iteration cycles. In Appendix E, the algorithm for the process is presented.

For the purpose of checking the algorithm, the range candidate, R_{G0}, is selected as shown in Figure 23. Actual ranges are chosen from 10 meters to 700 meters and R_{G0}'s are 700 meters for up to 350 meters of actual ranges and 10 meters for longer than 350 meters. This choice appears to correspond to worst-case guessing. The results for error calculation are obtained for $\theta =$ 0 degrees, 30 degrees, and 45 degrees at a detector height of 5 meters. The actual temperature and convergence parameter δ are chosen to be 353.54 K and 0.001, respectively. The error of range determination is shown in Figure 24, and the error of temperature determination is shown in Figure 25. Both errors in-

crease as the actual range increases. However, the maximum error in temperature and range is insignificantly small. The maximum error in ranging is 0.09 % and the maximum error in temperature is 0.0008 %. This results shows that the method performs remarkably well for the conditions tested.

In the calculation of the transmission factor for the i-th band, the precise τ_{ik} should be calculated according to the weighted average

$$\tau_{ik} = \frac{\int_{\lambda_{lower}}^{\lambda_{upper}} Q_\lambda(\lambda, T)\tau_{ik}(\lambda)d\lambda}{\int_{\lambda_{lower}}^{\lambda_{upper}} Q_\lambda(\lambda, T)d\lambda} \tag{5.27}$$

rather than the standard average (5.12). It should be noted that, the flatter the photon emittance distribution within the spectral bands, the smaller the discrepancy between calculations (5.12) and (5.27).

Despite the simplifying assumptions used in the model, the results demonstrate the feasibility of extracting both target range and temperature from thermal radiation measured over three bands.

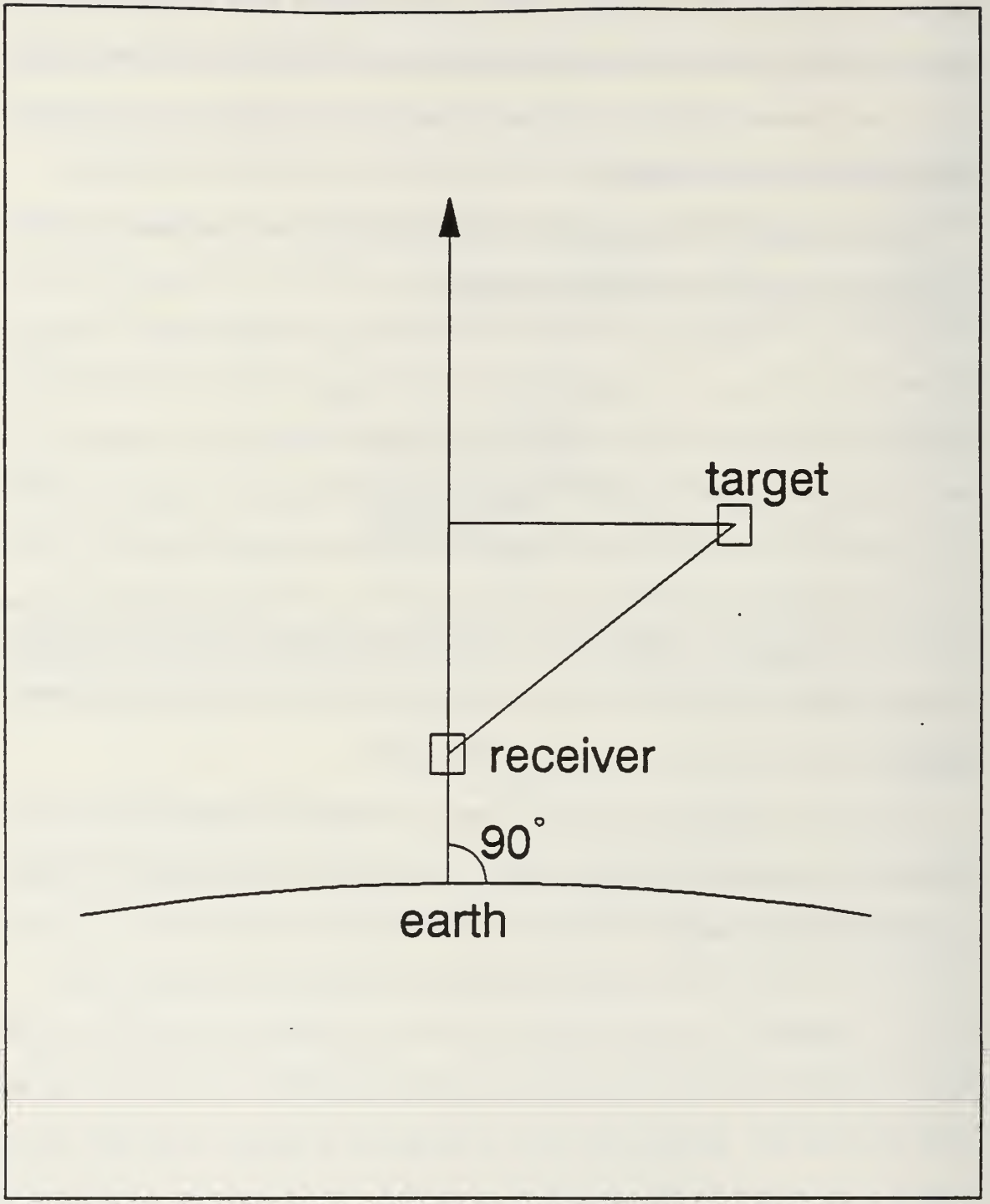

Figure 15. Definition of vertical line from the earth through the receiver

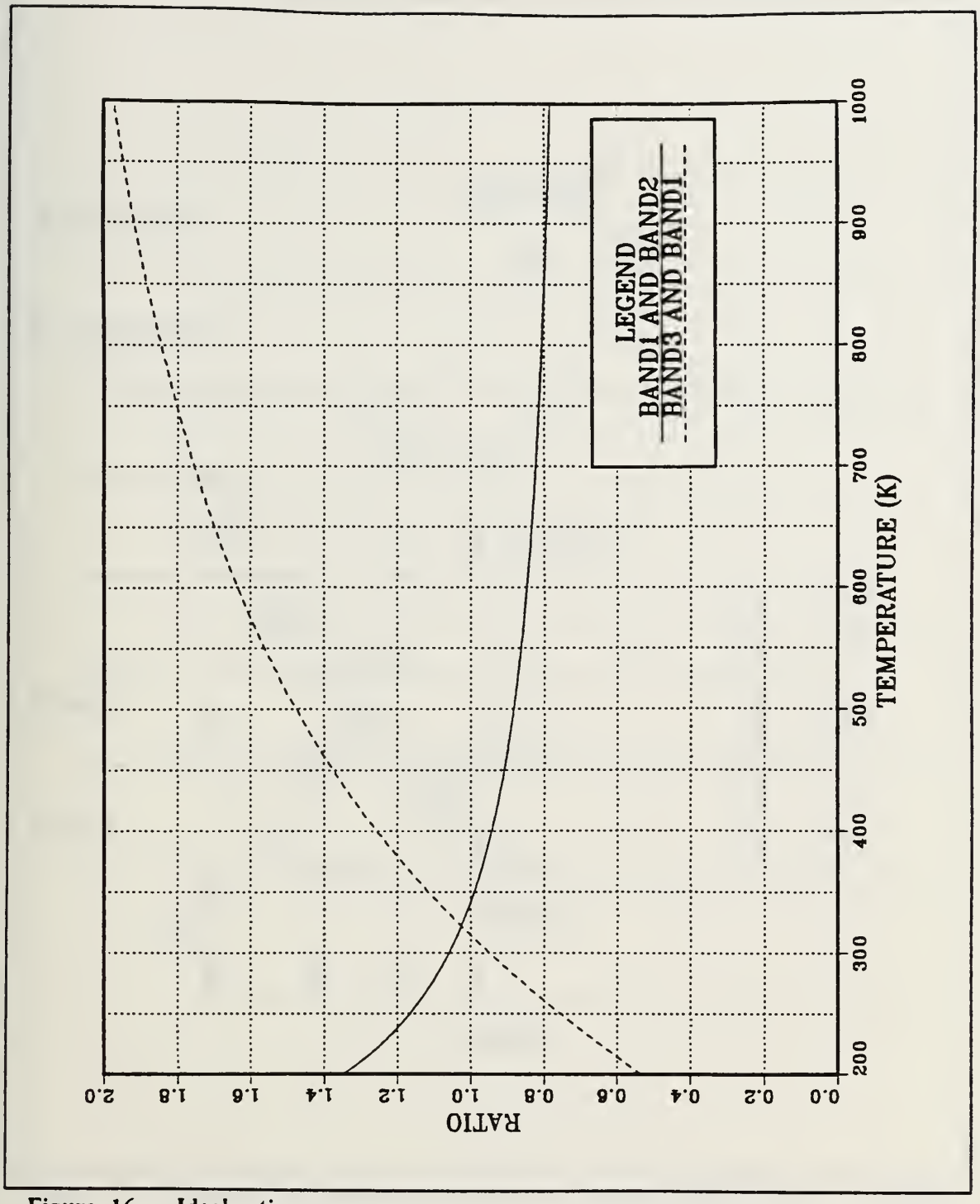

Figure 16. Ideal ratio curves

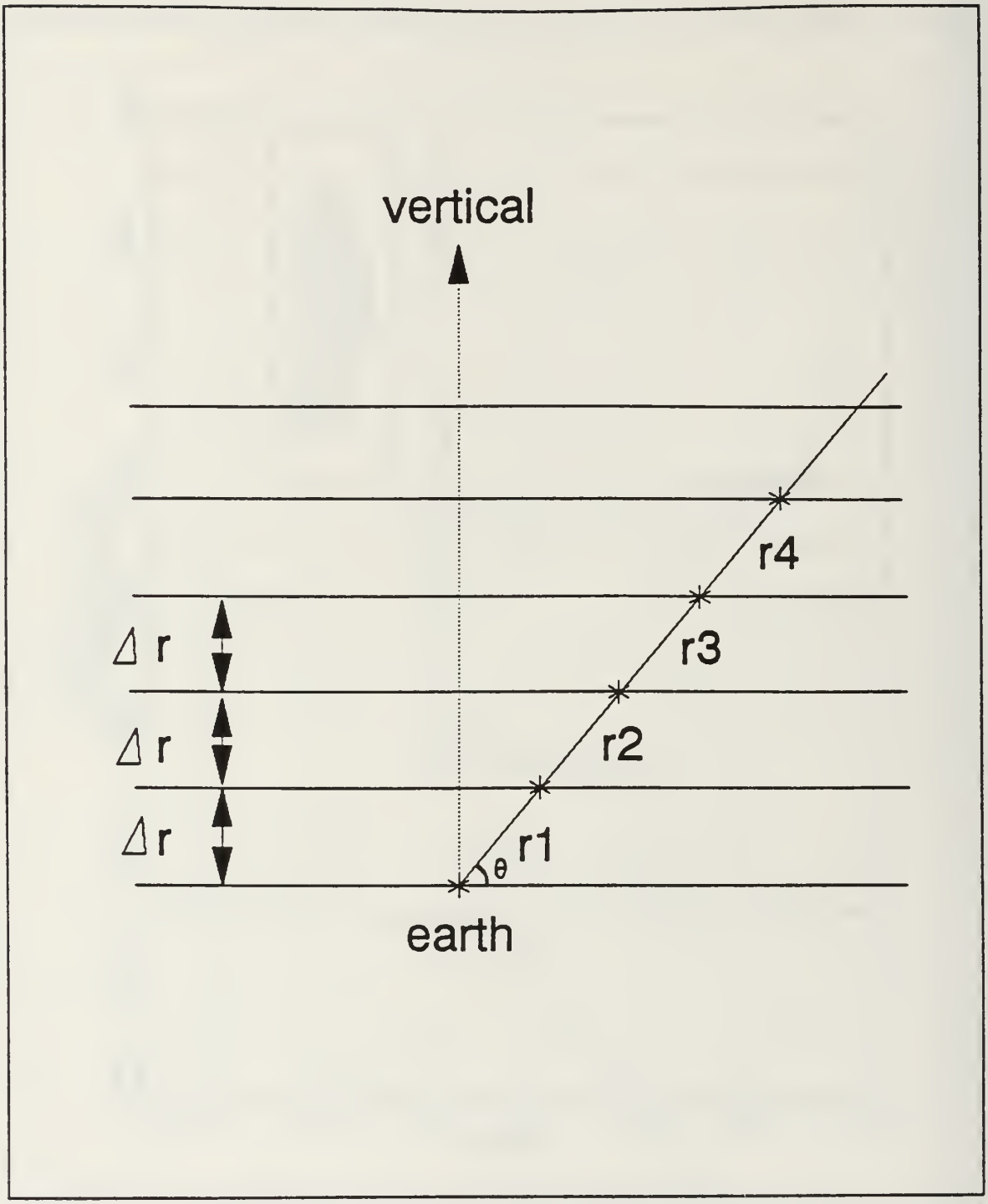

Figure 17. Definition of layers in atmosphere

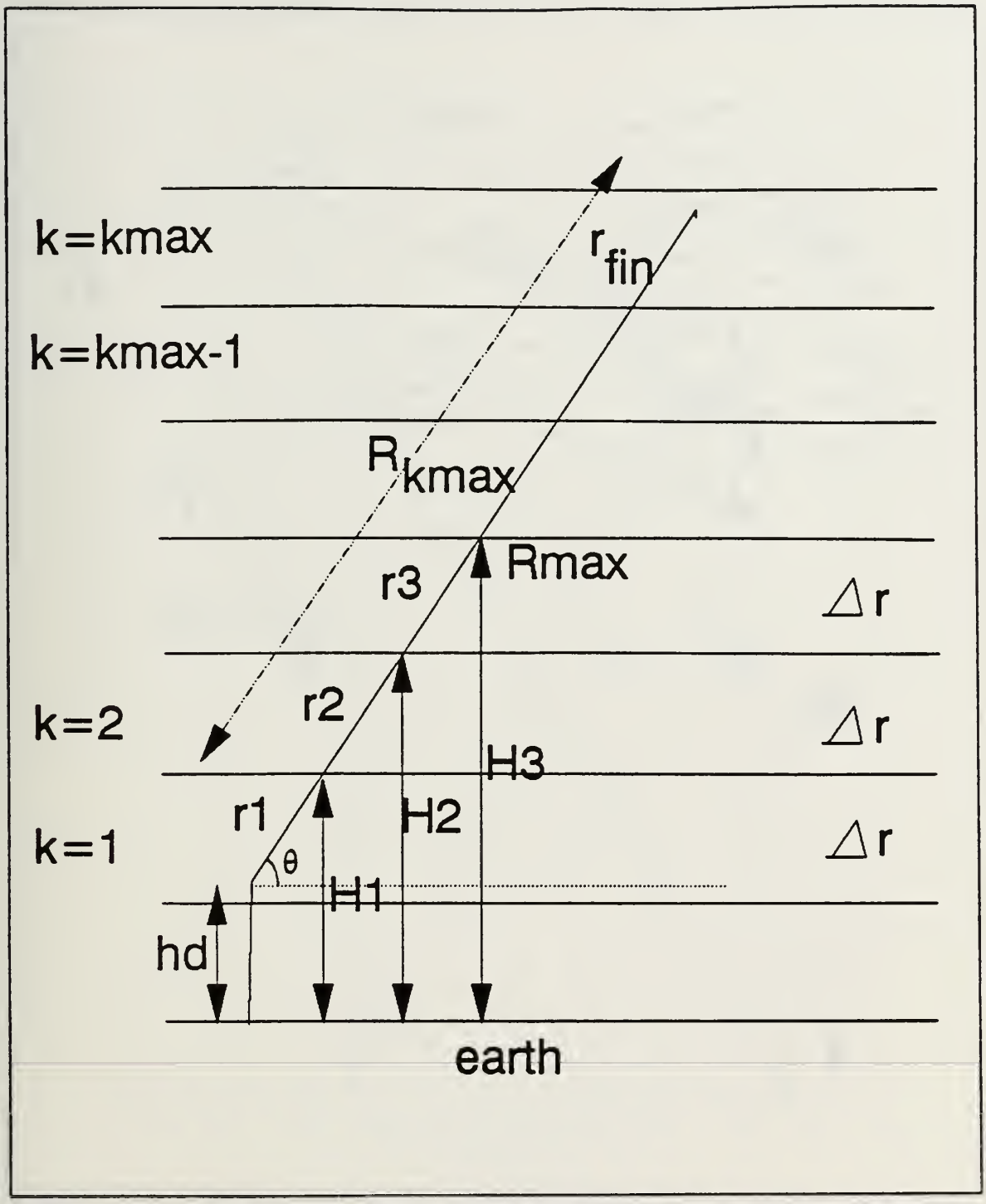

Figure 18. Layer of the atmosphere

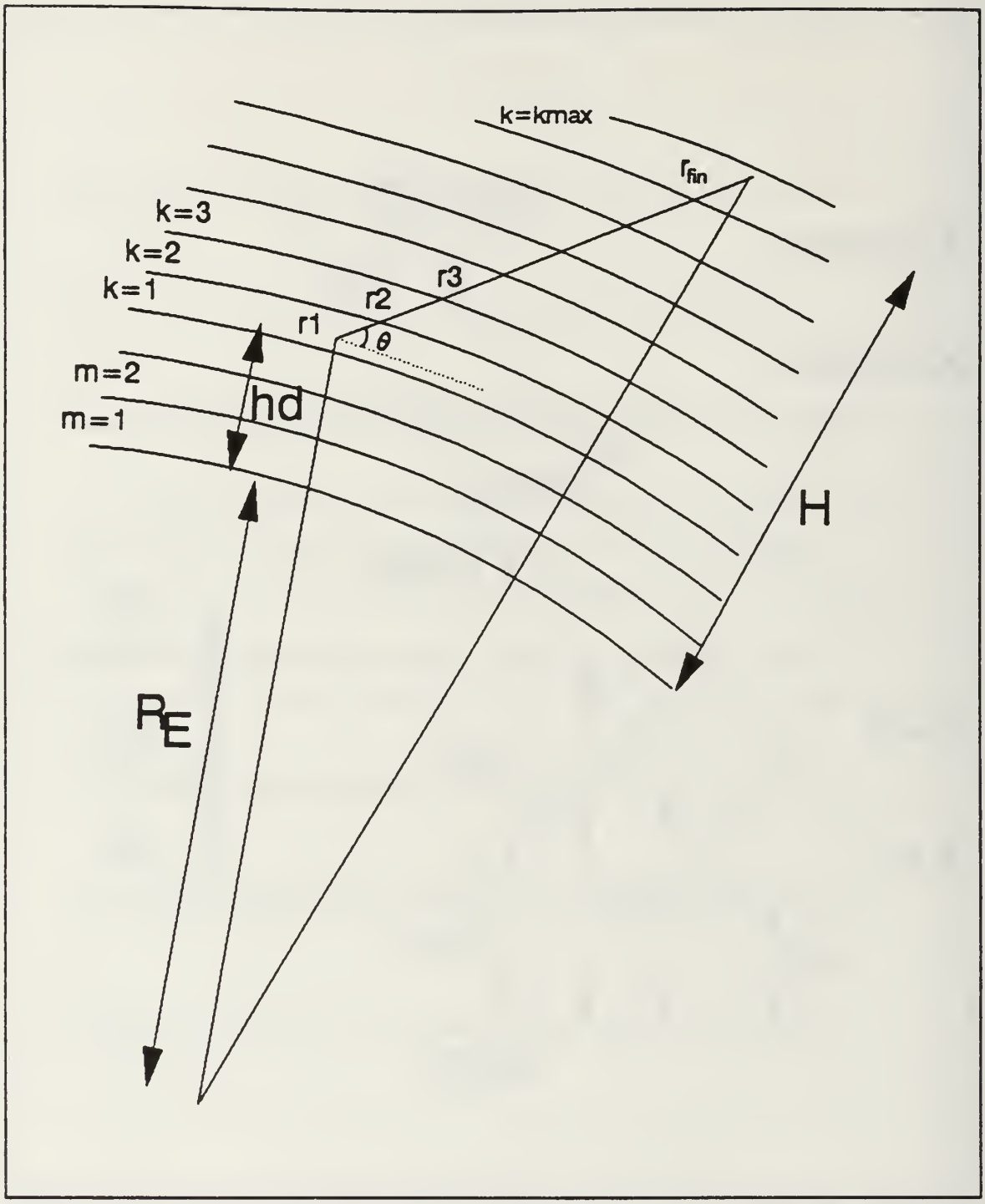

Figure 19. Geometry of ranging

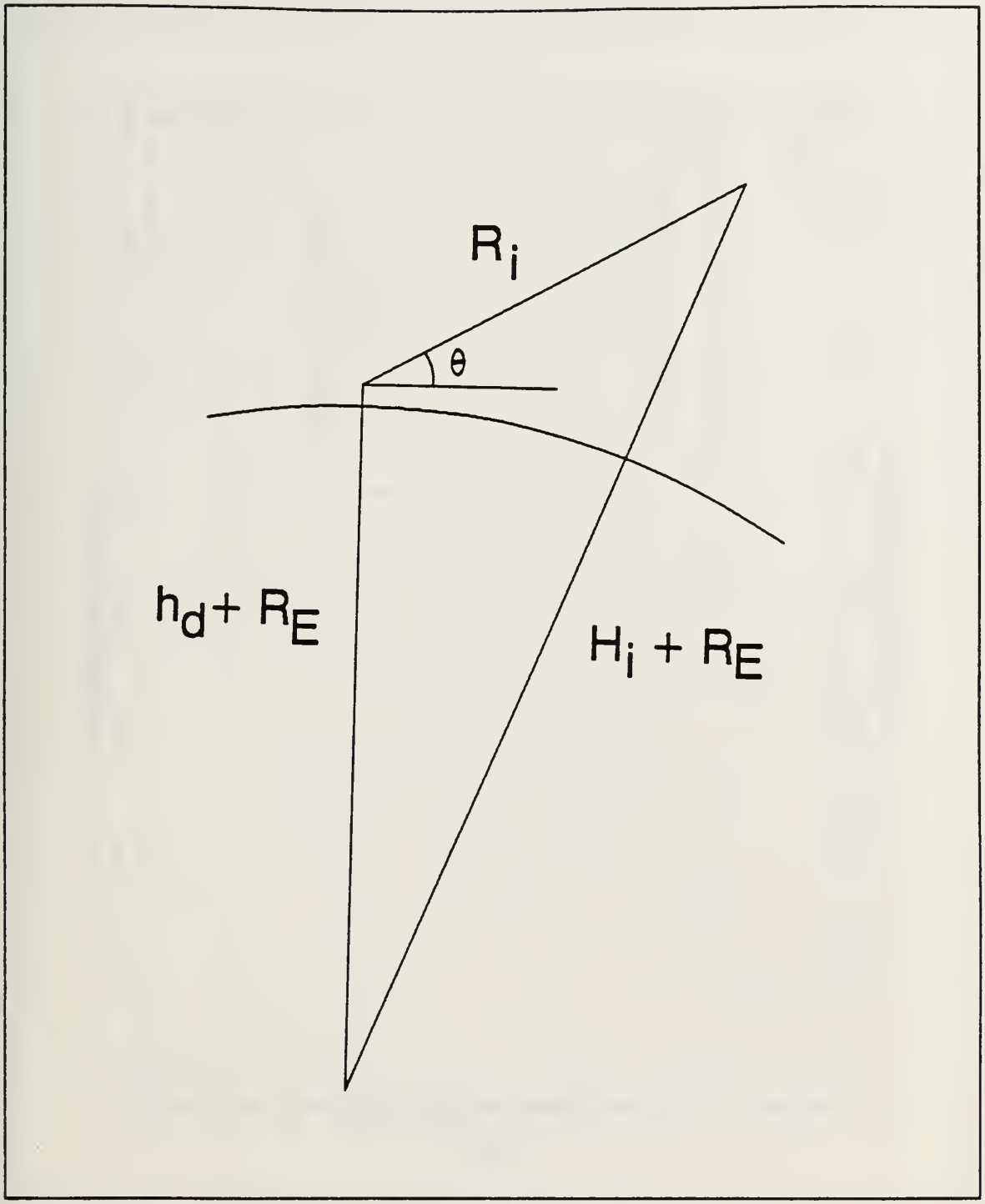

Figure 20. Geometry of ranging (cosine law)

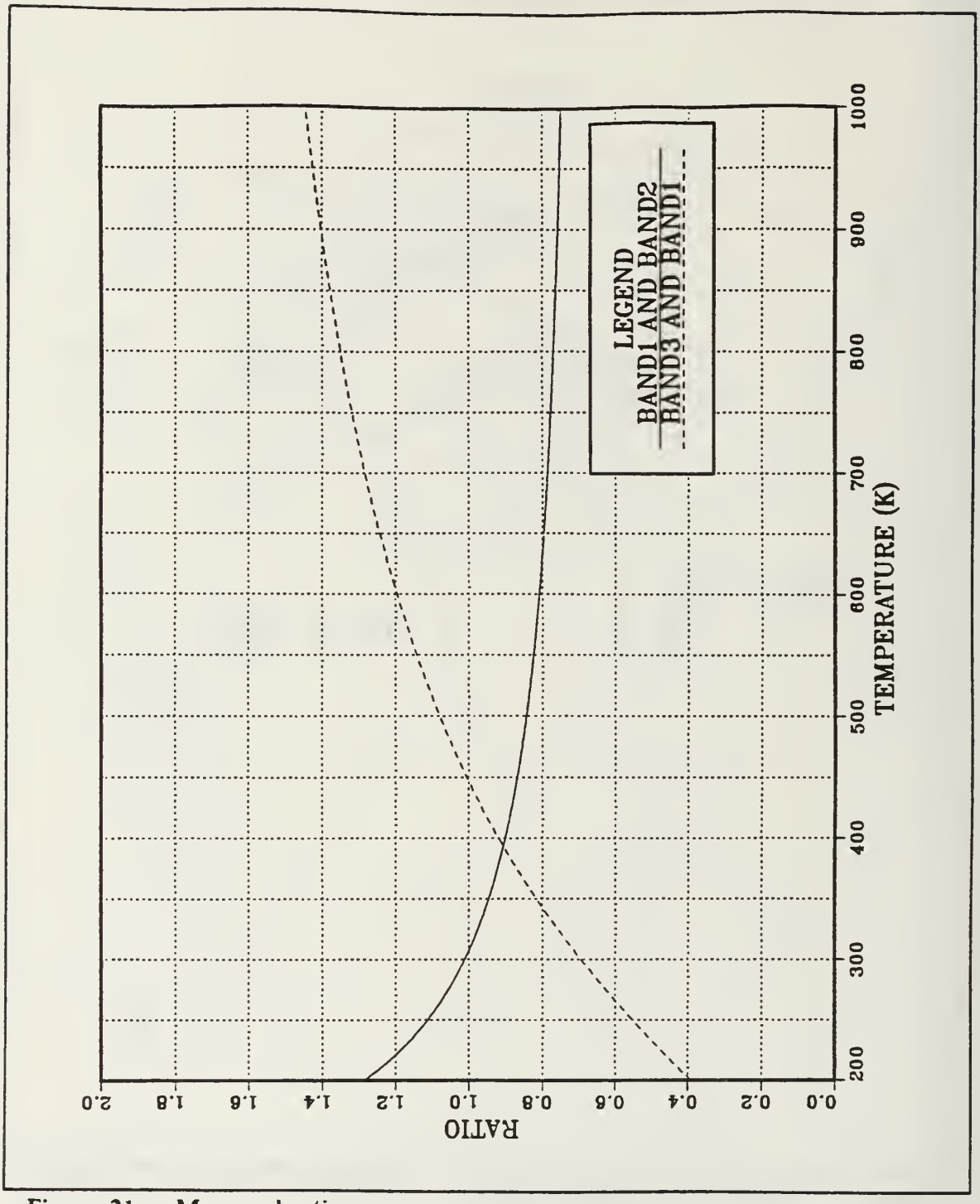

Figure 21. Measured ratio curves

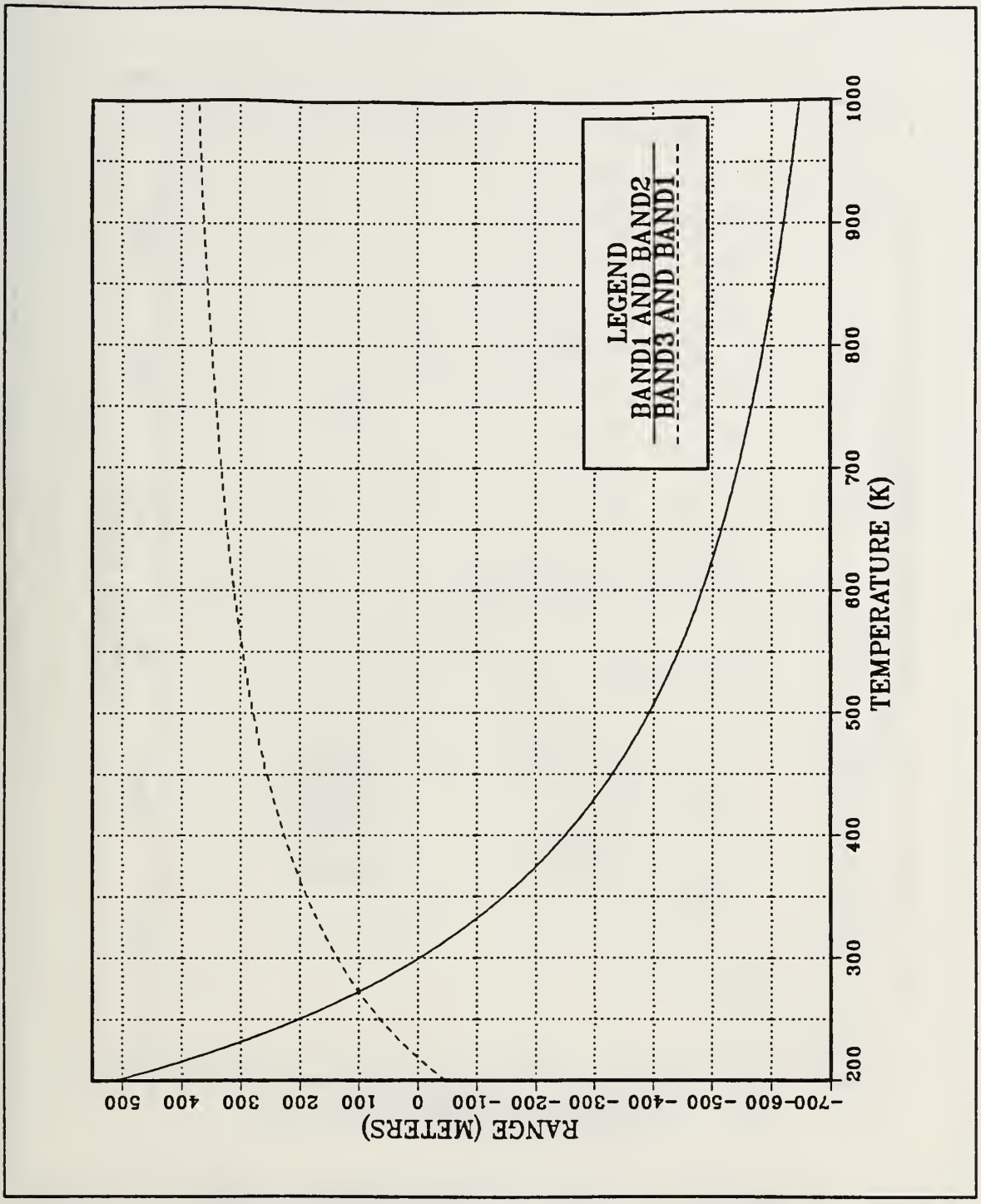

Figure 22. Graphical solution of range and temperature

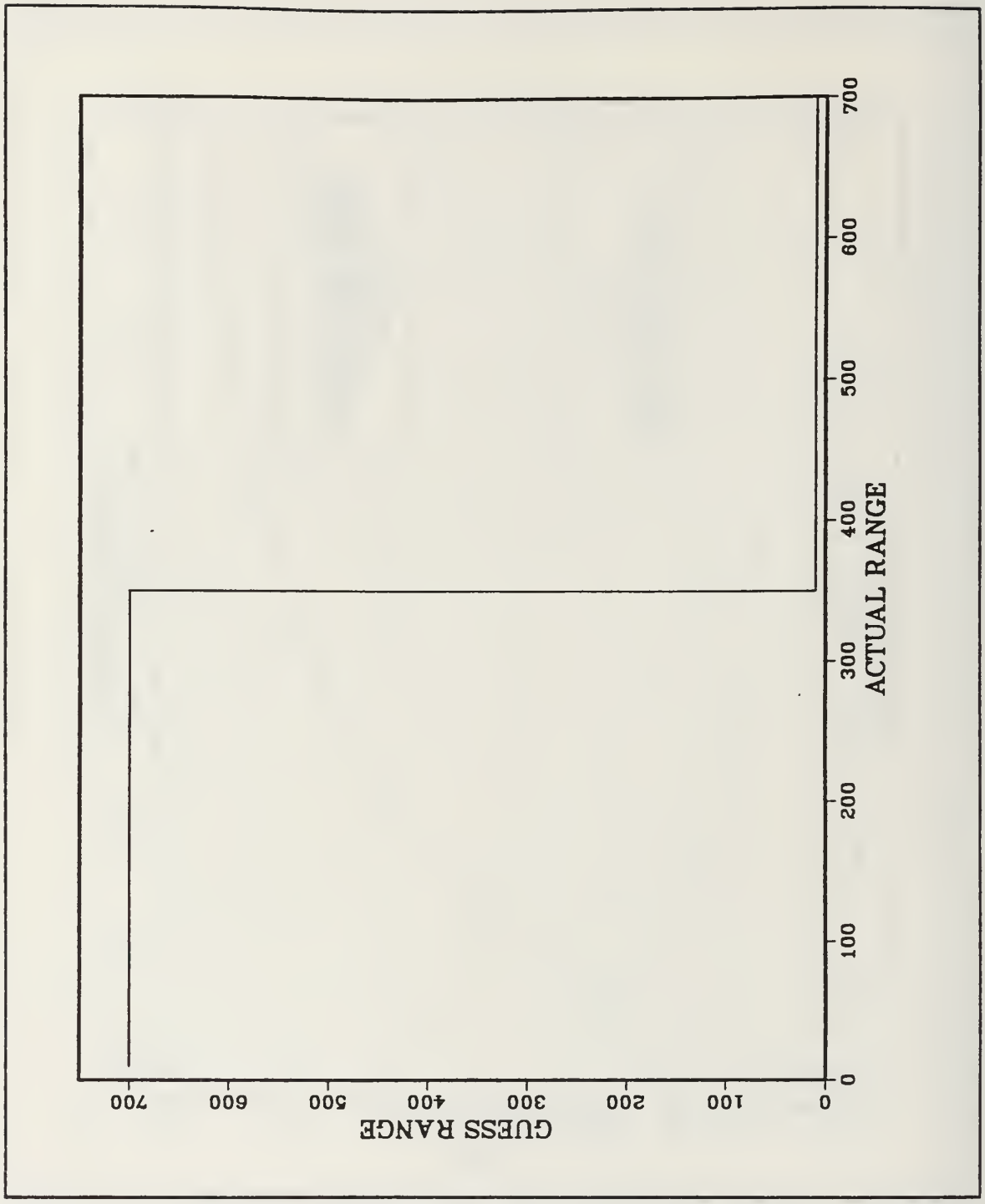

Figure 23. Initial guess range (the worst case)

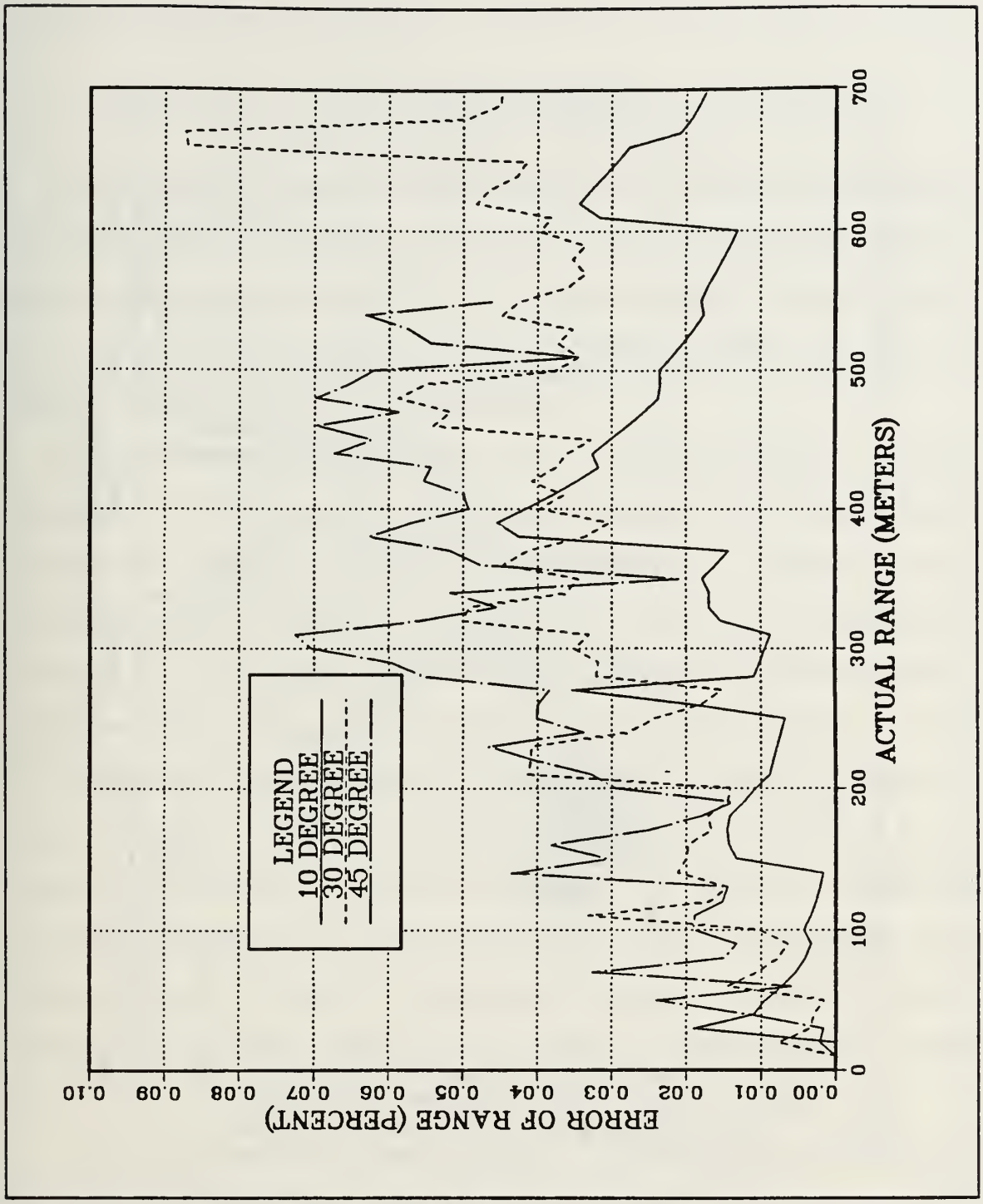

Figure 24. Error of range determination

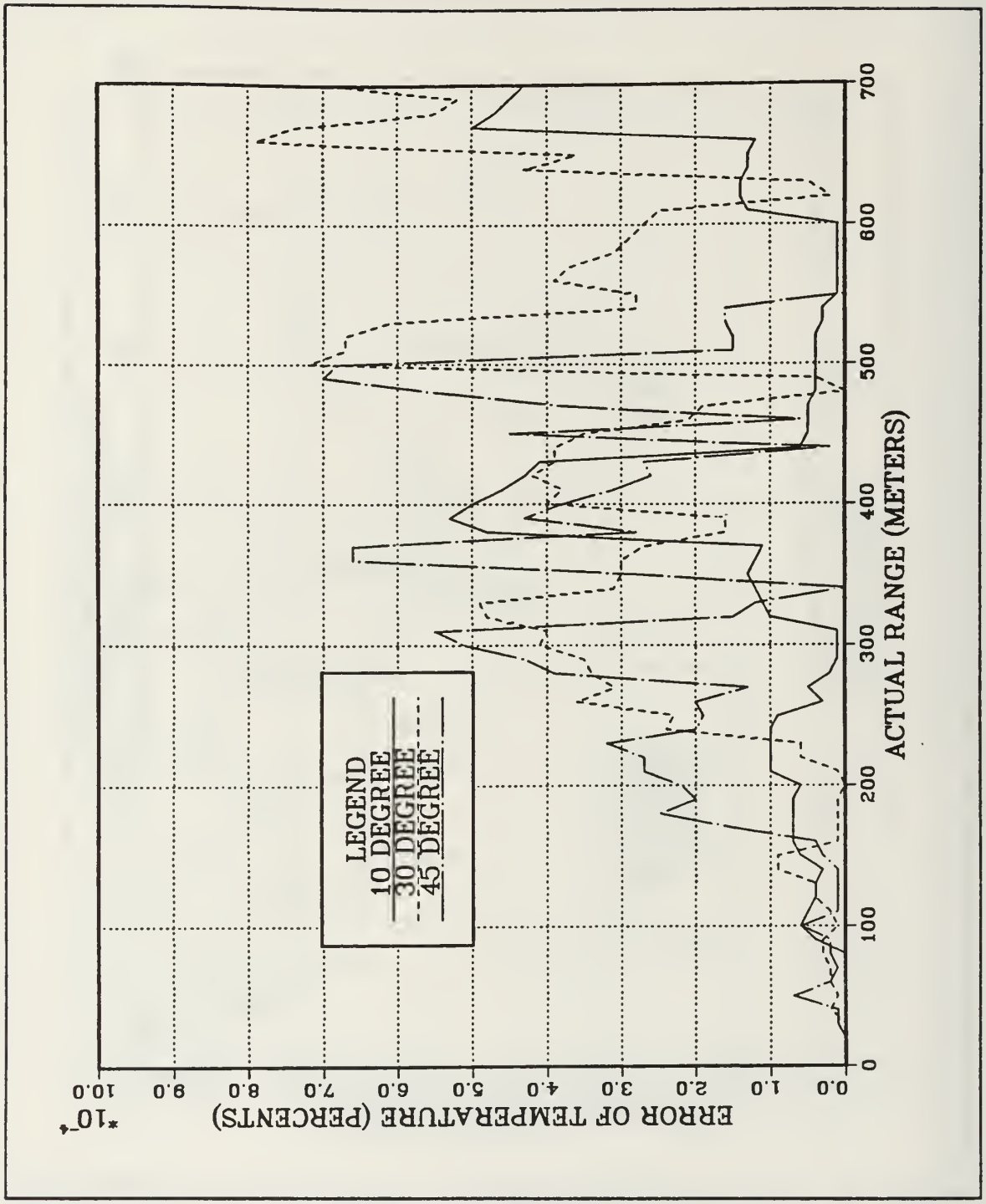

Figure 25. Error of temperature determination

VI. CONCLUSIONS

Previous work on dual spectral band measurements of radiant emittance demonstrated that, under somewhat ideal conditions, the ratio of the measurements could be used to determine the temperature. The main stipulated condition was that the bands were not self-contained. In the Chapter III of this thesis, the same conclusions were obtained for measurements of photon emittance.

A general model encompassing arbitrary wavelength-dependent emissivity, responsivity, and transmission factor was proposed in Chapter IV. Although the general problem is not analytically tractable, the methods applicable to constant emissivity, responsivity, and transmission factor (Chapter III) are approximately valid if the spectral bands are narrow enough. However, from the practical view point of making a signal measurement in the presence of noise, the spectral bands should not be too narrow. Therefore, the more general model is often needed under practical conditions. For reason explained in Chapter IV, the photon detector responsivity introduced is fairly insensitive to wavelength up to the cut-off wavelength. In addition, for a broad class of materials emissivity curves are quite flat. Therefore, the focus of the reminder of the thesis concentrated on effects due to atmospheric attenuation. Specifically, knowledge of the range to the target would be necessary to apply the method discussed in Chapter IV.

The concept presented and tested in Chapter V is created from the requirement that the dual spectral band method of temperature determination would require range information to determine the temperature. This assumes a disparity in attenuation effects between bands. By employing three bands instead of two, this problem is circumvented. Additional complications created by changing atmospheric conditions with trajectory

path are handled within the model. The numerical atmospheric attenuation data used in the model testing was taken from LOWTRAN. The results for this preliminary model are extremely encouraging. Future work needs to be performed to develop and test a more rigorous model.

APPENDIX A. DERIVATIVE OF $\mathscr{R}$ WITH RESPECT TO T

The purpose of this appendix is to prove equation (3.7) which appears in the main text. Equation (3.7) had been introduced in [Ref. 8: pp. 1257] without proof. Since the ratio of photon emittance is a function of α, it requires a few steps to get its derivative with respect T. For the reader's convenience, relations (3.2a), (3.5) and (3.6) are reproduced, which show that

$$\mathscr{R}_p = \frac{\int_{\alpha}^{\alpha x_2} g(\psi) d\psi}{\int_{\alpha x_3}^{\alpha x_4} g(\psi) d\psi} \tag{A1}$$

where

$$g(\psi) = \frac{\psi^2}{\exp(\psi) - 1} \tag{A2}$$

and

$$\alpha = \frac{T_r}{T}. \tag{A3}$$

Following the product rule, the derivative of the ratio of photon emittance (A1) with respect to temperature is

$$\frac{\partial \mathcal{R}}{\partial T} = \frac{\frac{\partial}{\partial T}\int_{\alpha}^{\alpha x_2} g(\psi)d\psi \int_{\alpha x_3}^{\alpha x_4} g(\psi)d\psi - \int_{\alpha}^{\alpha x_2} g(\psi)d\psi \frac{\partial}{\partial T}\int_{\alpha x_3}^{\alpha x_4} g(\psi)d\psi}{\left[\int_{\alpha x_3}^{\alpha x_4} g(\psi)d\psi\right]^2} \qquad (A4)$$

where the temperature dependence is expressed through α. One approach to simplifying the expression is to transfer the dependence of the integral limit on α evident in (A4) to the integrand. A substitution,

$$\psi = \alpha x \qquad (A5a)$$

will transfer this dependence. It follows that

$$\int_{\alpha x_i}^{\alpha x_j} g(\psi)d\psi = \alpha \int_{x_i}^{x_j} g(\alpha x)dx. \qquad (A5b)$$

Therefore according to the product rule,

$$\frac{\partial}{\partial \alpha}\int_{\alpha x_i}^{\alpha x_j} g(\psi)d\psi = \int_{x_i}^{x_j} g(\alpha x)dx + \alpha \int_{x_i}^{x_j} \frac{\partial}{\partial \alpha} g(\alpha x)dx. \qquad (A6)$$

Now from (A2) and the transformation rule (A5a),

$$g(\alpha x) = \frac{(\alpha x)^2}{\exp(\alpha x) - 1}, \qquad (A7)$$

and it follows from (A7) that

$$\frac{\partial}{\partial \alpha} g(\alpha x) = \frac{2\alpha x^2}{\exp(\alpha x) - 1} - \frac{\alpha^2 x^3 \exp(\alpha x)}{[\exp(\alpha x) - 1]^2}. \qquad (A8)$$

Direct substitution of (A8) into (A6) leads to :

$$\frac{\partial}{\partial \alpha} \int_{\alpha x_i}^{\alpha x_j} g(\psi) d\psi = \int_{x_i}^{x_j} g(\alpha x) dx + \int_{x_i}^{x_j} \frac{2(\alpha x)^2}{\exp(\alpha x) - 1} dx - \int_{x_i}^{x_j} \frac{(\alpha x)^3 \exp(\alpha x)}{[\exp(\alpha x) - 1]^2} dx. \qquad (A9)$$

Noting the equivalence between $g(\alpha x)$ defined in (A7), and the integrand of the second integral (A9), it follows that :

$$\frac{\partial}{\partial \alpha} \int_{\alpha x_i}^{\alpha x_j} g(\psi) d\psi = 3 \int_{x_i}^{x_j} g(\alpha x) dx - \int_{x_i}^{x_j} \frac{(\alpha x)^3 \exp(\alpha x)}{[\exp(\alpha x) - 1]^2} dx. \qquad (A10)$$

After reversing the transformation (A5a), the integrands in (A10) will depend on ψ and (A10) leads to:

$$\frac{\partial}{\partial \alpha} \int_{\alpha x_i}^{\alpha x_j} g(\psi) d\psi = \frac{3}{\alpha} \int_{\alpha x_i}^{\alpha x_j} g(\psi) d\psi - \frac{1}{\alpha} \int_{\alpha x_i}^{\alpha x_j} \frac{\psi^3 \exp(\psi)}{[\exp(\psi) - 1]^2} d\psi. \qquad (A11)$$

For compactness of representation, define

$$f(\psi) = \frac{\psi^3 \exp(\psi)}{[\exp(\psi) - 1]^2}. \qquad (A12)$$

Then combining the result (A3) with (A11) leads to :

$$\frac{\partial}{\partial T}\int_{\alpha x_i}^{\alpha x_j} g(\psi)d\psi = \frac{1}{T}\left[\int_{\alpha x_i}^{\alpha x_j} f(\psi)d\psi - 3\int_{\alpha x_i}^{\alpha x_j} g(\psi)d\psi\right]. \qquad (A13)$$

After substituting (A13) into (A4)

$$\frac{\partial \mathcal{R}_p}{\partial T} = \frac{1}{T}\frac{\left[\int_{\alpha}^{\alpha x_2} f(\psi)d\psi - 3\int_{\alpha}^{\alpha x_2} g(\psi)d\psi\right]\int_{\alpha x_3}^{\alpha x_4} g(\psi)d\psi - \int_{\alpha}^{\alpha x_2} g(\psi)d\psi\left[\int_{\alpha x_3}^{\alpha x_4} f(\psi)d\psi - 3\int_{\alpha x_3}^{\alpha x_4} g(\psi)d\psi\right]}{\left[\int_{\alpha x_3}^{\alpha x_4} g(\psi)d\psi\right]^2},$$

(A14)

which after simplification leads directly to (A16) or (3.7), as given in the text.

$$\frac{\partial \mathcal{R}_p}{\partial T} = \frac{1}{T}\frac{\int_{\alpha}^{\alpha x_2} f(\psi)d\psi\int_{\alpha x_3}^{\alpha x_4} g(\psi)d\psi - \int_{\alpha}^{\alpha x_2} g(\psi)d\psi\int_{\alpha x_3}^{\alpha x_4} f(\psi)d\psi}{\left[\int_{\alpha x_3}^{\alpha x_4} g(\psi)d\psi\right]^2} \qquad (A15)$$

APPENDIX B. ASYMPTOTIC APPROXIMATION FOR RATIO CALCULATION

The purpose of this appendix is to prove equations (3.22) and (3.23) which appear in the main text where the asymptotic approximations are applied.

A. FOR LARGE ALPHA

For large α (i.e., small temperature), since x_i values are fixed, ψ takes on large positive values Therefore, $g(\psi)$ and $f(\psi)$ functions are approximated from (3.5) and (3.8) as follows:

$$g(\psi) \simeq \frac{\psi^2}{\exp(\psi)} \tag{B1}$$

and

$$f(\psi) \simeq \frac{\psi^3}{\exp(\psi)} . \tag{B2}$$

After direct substitution into (3.8), it follows that:

$$\begin{aligned} [f,g] \simeq & \int_{\alpha}^{\alpha x_2} \psi^3 \exp(-\psi) d\psi \int_{\alpha x_3}^{\alpha x_4} \psi^2 \exp(-\psi) d\psi \\ & - \int_{\alpha}^{\alpha x_2} \psi^2 \exp(-\psi) d\psi \int_{\alpha x_3}^{\alpha x_4} \psi^3 \exp(-\psi) d\psi \end{aligned} . \tag{B3}$$

One round of integration by parts yields

$$[f,g]\simeq\left\{\left[-\psi^3\exp(-\psi)\right]_{\alpha}^{\alpha x_2}+3\int_{\alpha}^{\alpha x_2}\psi^2\exp(-\psi)d\psi\right\}\int_{\alpha x_3}^{\alpha x_4}\psi^2\exp(-\psi)d\psi$$
$$-\int_{\alpha}^{\alpha x_2}\psi^2\exp(-\psi)d\psi\left\{\left[-\psi^3\exp(-\psi)\right]_{\alpha x_3}^{\alpha x_4}+3\int_{\alpha x_3}^{\alpha x_4}\psi^2\exp(-\psi)d\psi\right\}. \qquad (B4)$$

After algebraic simplification, (B4) becomes

$$[f,g]\simeq\left[-\psi^3\exp(-\psi)\right]_{\alpha}^{\alpha x_2}\int_{\alpha x_3}^{\alpha x_4}\psi^2\exp(-\psi)d\psi$$
$$-\int_{\alpha}^{\alpha x_2}\psi^2\exp(-\psi)d\psi\left[-\psi^3\exp(-\psi)\right]_{\alpha x_3}^{\alpha x_4}. \qquad (B5)$$

According to [Ref. 12: pp. 85]

$$\int\psi^2\exp(-\psi)d\psi=-\psi^2\exp(-\psi)-2\psi\exp(-\psi)-2\exp(-\psi), \qquad (B6)$$

which, for large positive ψ (B6), is approximately given by

$$\int\psi^2\exp(-\psi)d\psi\simeq-\psi^2\exp(-\psi). \qquad (B7)$$

After substitution of the approximate form (B7) into the integrals (B5), [f,g] becomes

$$[f,g]\simeq[\psi^3\exp(-\psi)]_{\alpha}^{\alpha x_2}[\psi^2\exp(-\psi)]_{\alpha x_3}^{\alpha x_4}-[\psi^2\exp(-\psi)]_{\alpha}^{\alpha x_2}[\psi^3\exp(-\psi)]_{\alpha x_3}^{\alpha x_4}. \quad (B8)$$

which, after simplification, becomes

$$\begin{aligned}[f,g]\simeq&[(\alpha x_2)^3\exp(-\alpha x_2)-\alpha^3\exp(-\alpha)][(\alpha x_4)^2\exp(-\alpha x_4)-(\alpha x_3)^2\exp(-\alpha x_3)]\\&-[(\alpha x_2)^2\exp(-\alpha x_2)-\alpha^2\exp(-\alpha)][(\alpha x_4)^3\exp(-\alpha x_4)-(\alpha x_3)^3\exp(-\alpha x_3)]\end{aligned} \quad (B9)$$

Since, for large α, the second terms within each bracket of (B9) become dominant, [f,g] is approximated as

$$[f,g]\simeq\alpha^5[x_3^2\exp(-\alpha x_3)\exp(-\alpha)-x_3^3\exp(-\alpha x_3)\exp(-\alpha)]. \quad (B10)$$

Recombination of (B11) leads to:

$$[f,g]\simeq\alpha^5 x_3^2(1-x_3)\exp[-\alpha(x_3+1)]. \quad (B11)$$

This last form is applied in Section C of Chapter III.

B. FOR SMALL ALPHA

For small α (i.e., large temperature), ψ is small. Thus, $g(\psi)$ and $f(\psi)$ are approximated from (3.5) and (3.8) by binomial expansion. After application of binomial expansion, $g(\psi)$ is integrated as

$$\int g(\psi)d\psi\simeq\int\psi\left(1+\frac{\psi}{2}\right)^{-1}d\psi. \quad (B12)$$

And a binomial approximation for small ψ leads to:

$$\int g(\psi)d\psi\simeq\int\psi\left(1-\frac{\psi}{2}\right)d\psi, \quad (B13)$$

which is integrated as

$$\int g(\psi)d\psi \simeq \psi^2\left(\frac{1}{2} - \frac{\psi}{6}\right). \tag{B14}$$

Similarly, after applying binomial expansion to (3.8), the integration of $f(\psi)$ becomes

$$\int f(\psi)d\psi \simeq \int \psi(1+\psi)\left(1 - \frac{\psi}{2}\right)^2 d\psi. \tag{B15}$$

Algebraic expansion of (B15) leads to:

$$\int f(\psi)d\psi \simeq \int \psi^2\left(\frac{1}{2} - \frac{3}{16}\psi^2 + \frac{1}{20}\psi^3\right), \tag{B16}$$

which is approximated as

$$\int f(\psi)d\psi \simeq \psi^2\left(\frac{1}{2} - \frac{3}{16}\psi^2\right). \tag{B17}$$

Therefore, for small α, [f,g] becomes

$$\begin{aligned}[f,g] \simeq &\left[\psi^2\left(\frac{1}{2} - \frac{3}{16}\psi^2\right)\right]_{\alpha}^{\alpha x_2}\left[\psi^2\left(\frac{1}{2} - \frac{\psi}{6}\right)\right]_{\alpha x_3}^{\alpha x_4} \\ &- \left[\psi^2\left(\frac{1}{2} - \frac{\psi}{6}\right)\right]_{\alpha}^{\alpha x_2}\left[\psi^2\left(\frac{1}{2} - \frac{3}{16}\psi^2\right)\right]_{\alpha x_3}^{\alpha x_4},\end{aligned} \tag{B18}$$

which is expanded as

$$[f,g] \simeq \frac{\alpha^5}{12}(x_2^2-1)(x_4^3-x_3^3) - \frac{3}{32}\alpha^6(x_2^4-1)(x_4^2-x_3^2) - \frac{\alpha^7}{32}(x_2^4-1)(x_4^3-x_3^3)$$
$$- \frac{\alpha^5}{12}(x_4^2-x_3^2)(x_2^3-1) + \frac{3}{32}\alpha^6(x_4^4-x_3^4)(x_2^2-1) - \frac{\alpha^7}{32}(x_4^4-x_3^4)(x_2^3-1) \quad (B19)$$

Since, for small alpha, α^5 terms are dominant, [f,g] approximated as

$$[f,g] \simeq \frac{\alpha^5}{12}\left[(x_4^2-x_3^2)(x_2^3-1) - (x_2^2-1)(x_4^3-x_3^3)\right]. \quad (B20)$$

This final form is applied in Section C of Chapter III.

APPENDIX C. ALGORITHM TO CALCULATE THE RATIO OF PHOTON EMITTANCE

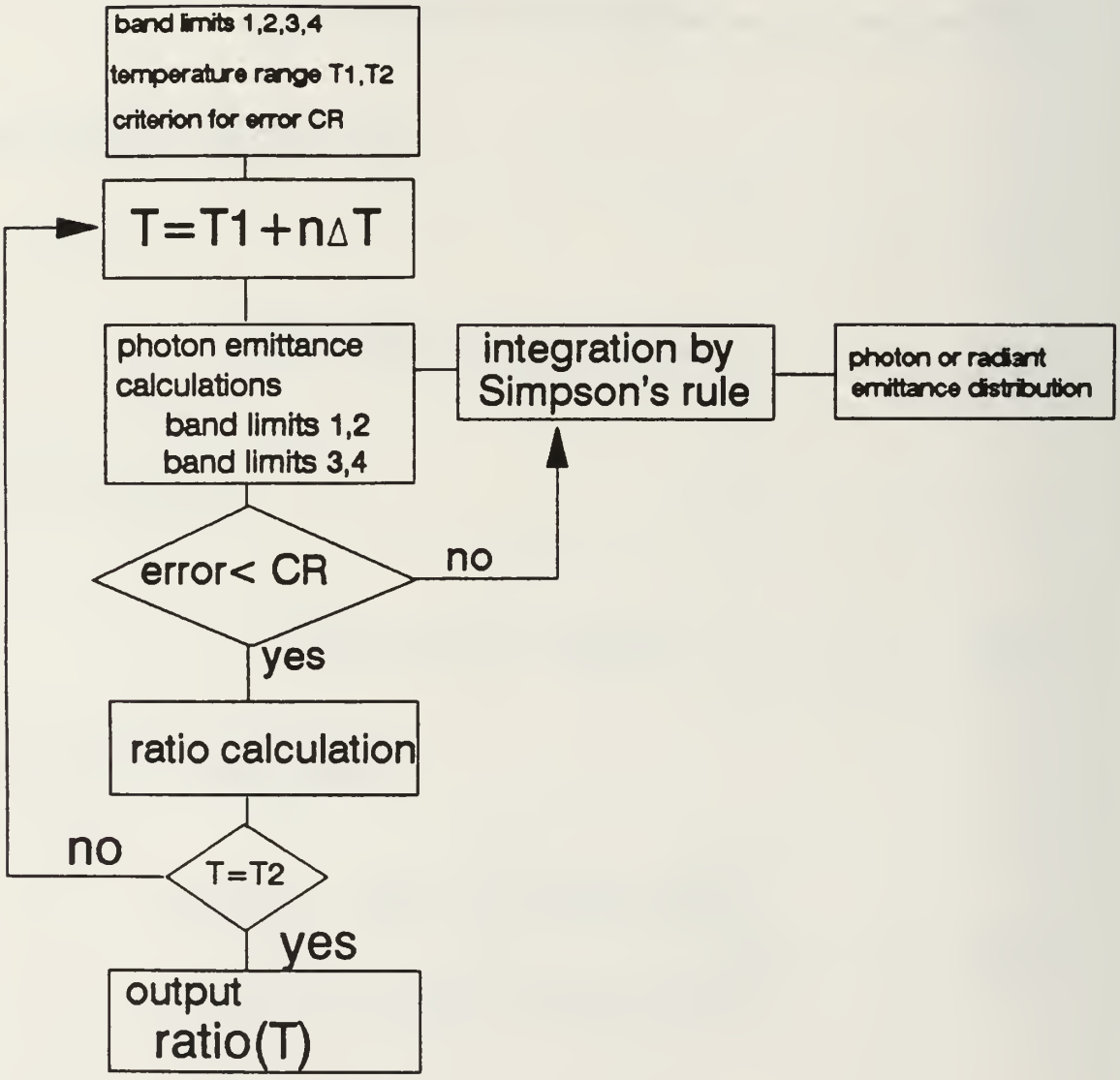

APPENDIX D. ALGORITHM TO CALCULATE THE RATIO OF OUTPUT VOLTAGE AT THE DETECTOR

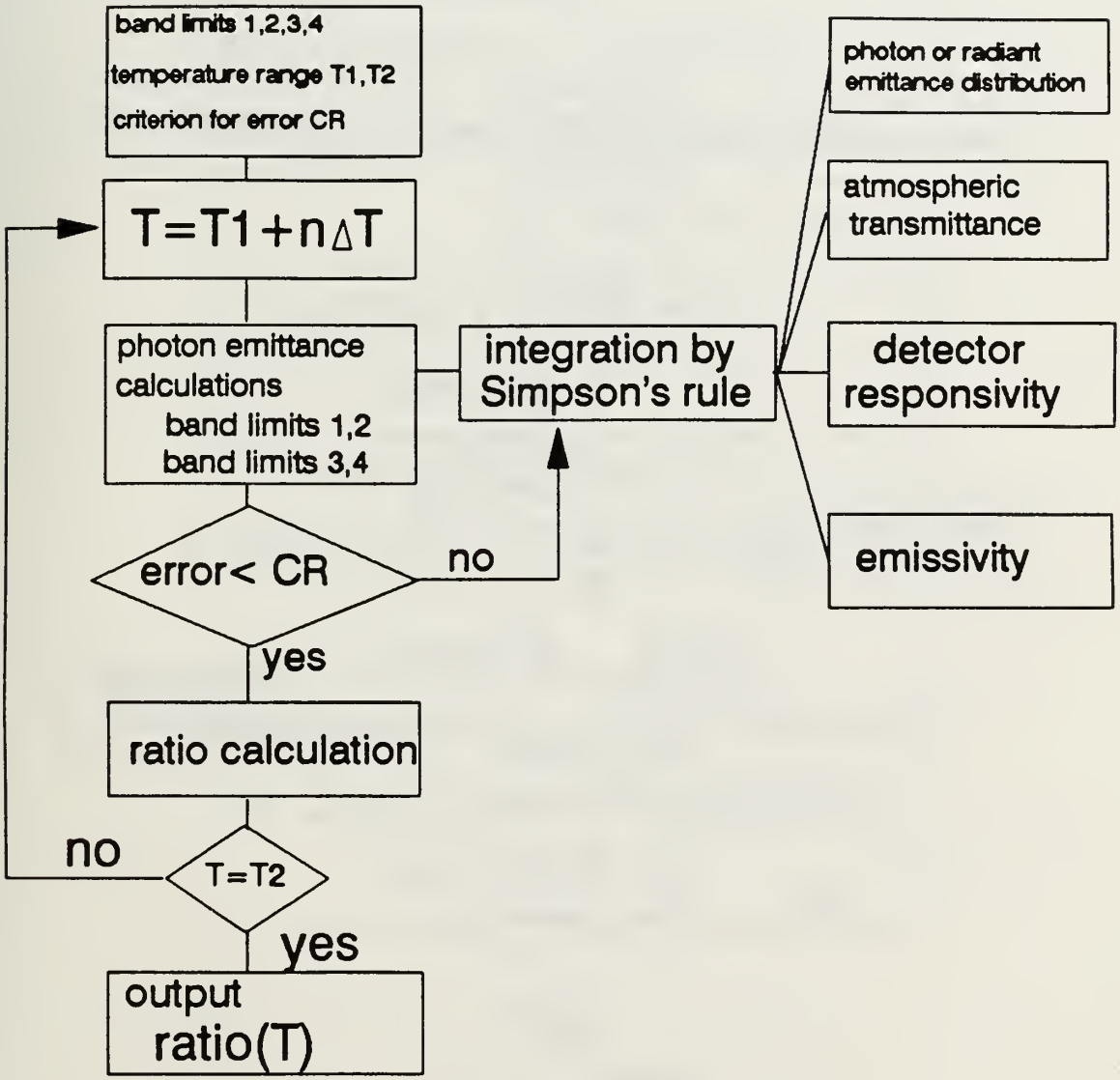

APPENDIX E. MODEL FOR PASSIVE RANGE AND TEMPERATURE DETERMINATION

A. MAIN ALGORITHM

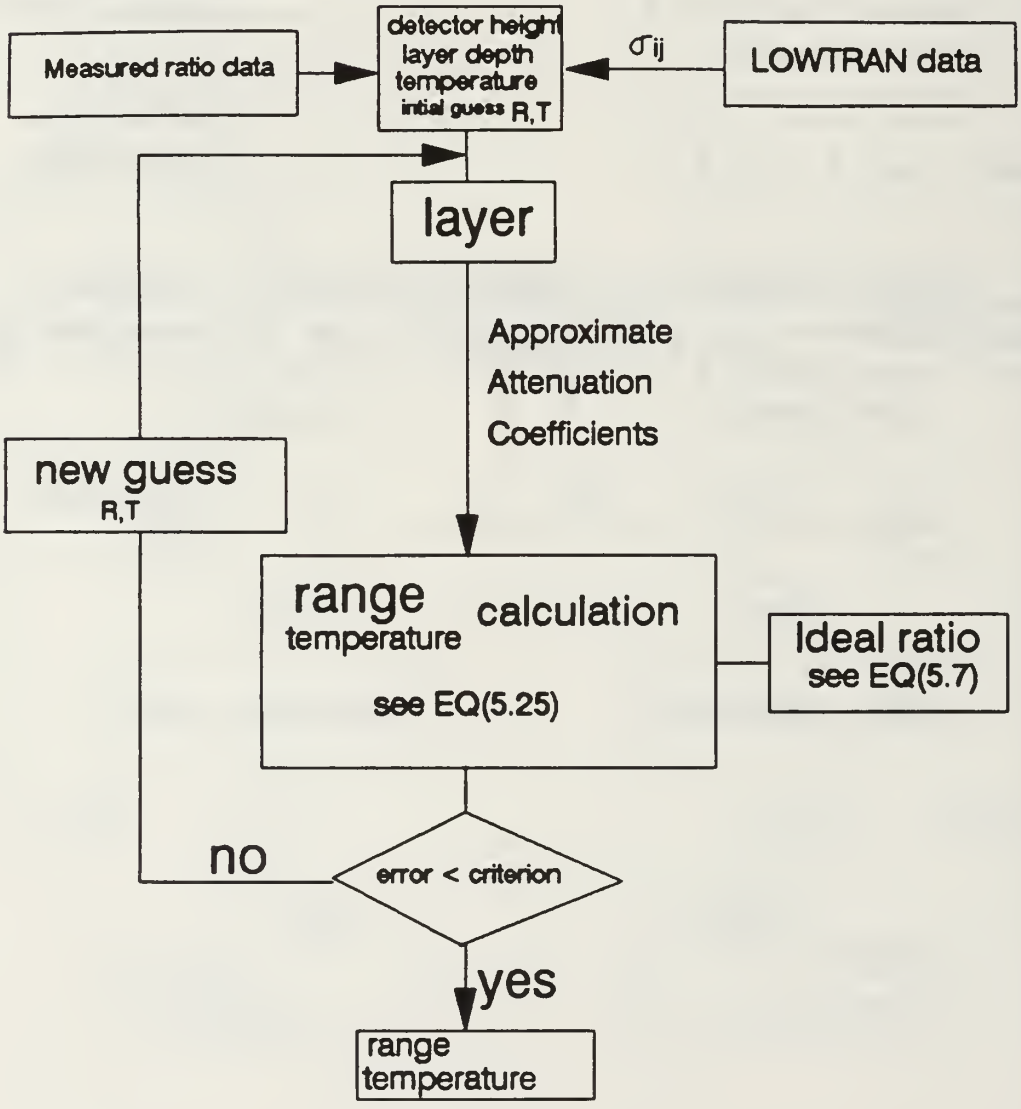

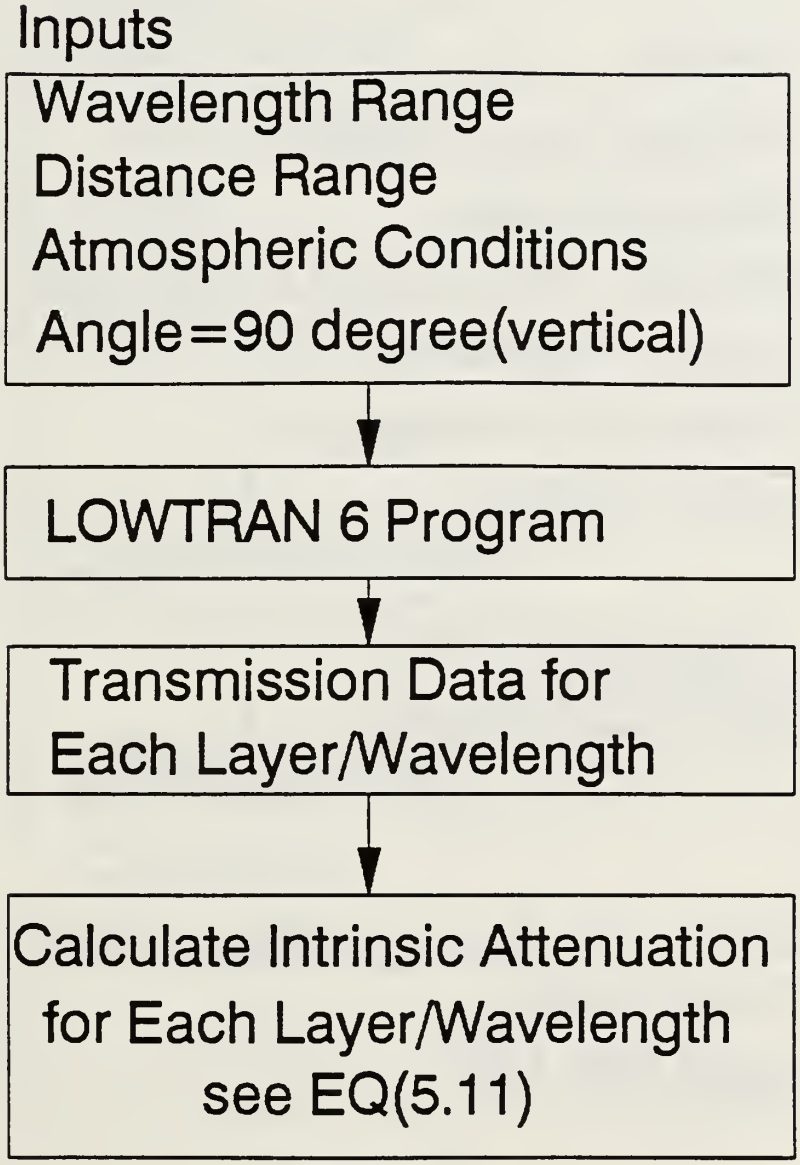
Inputs
Wavelength Range
Distance Range
Atmospheric Conditions
Angle=90 degree(vertical)
LOWTRAN 6 Program
Transmission Data for
Each Layer/Wavelength
Calculate Intrinsic Attenuation
for Each Layer/Wavelength
see EQ(5.11)

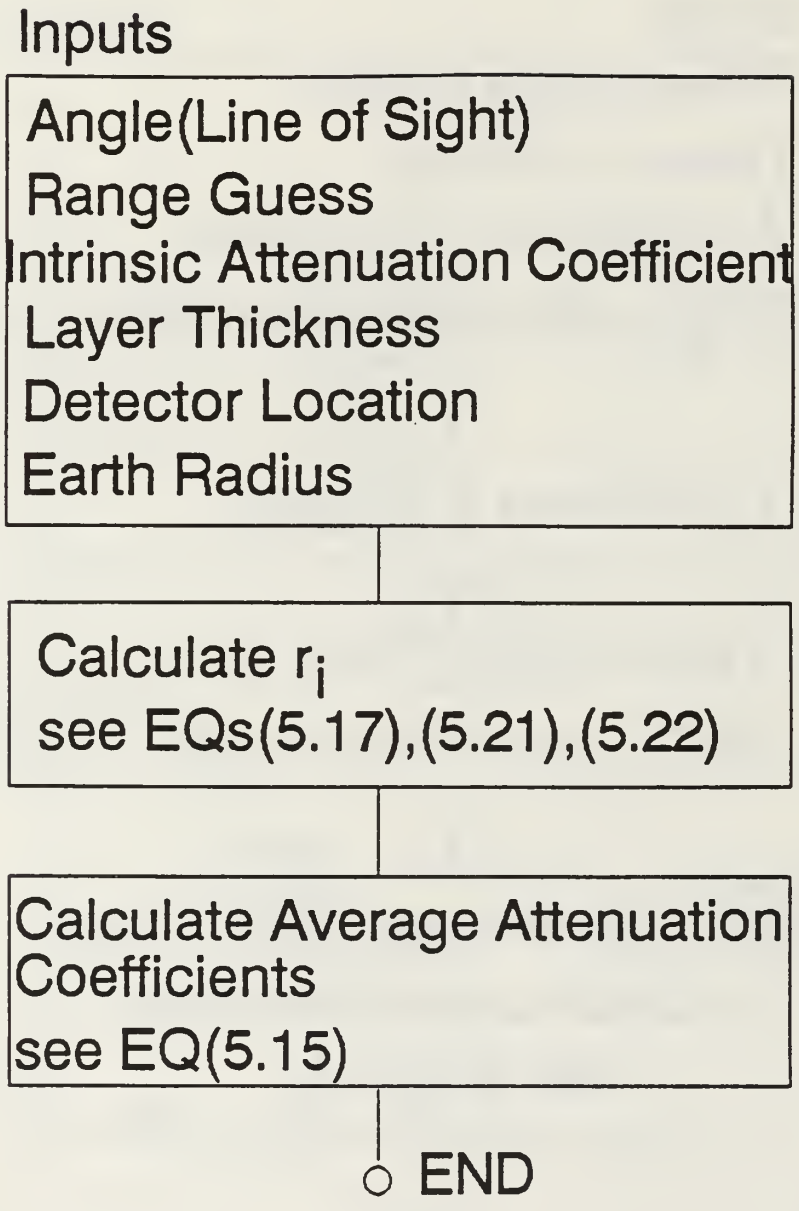
Inputs
Angle(Line of Sight)
Range Guess
Intrinsic Attenuation Coefficient
Layer Thickness
Detector Location
Earth Radius
Calculate r_i
see EQs(5.17),(5.21),(5.22)
Calculate Average Attenuation Coefficients
see EQ(5.15)
END

D. MEASURED RATIO PREDICTOR

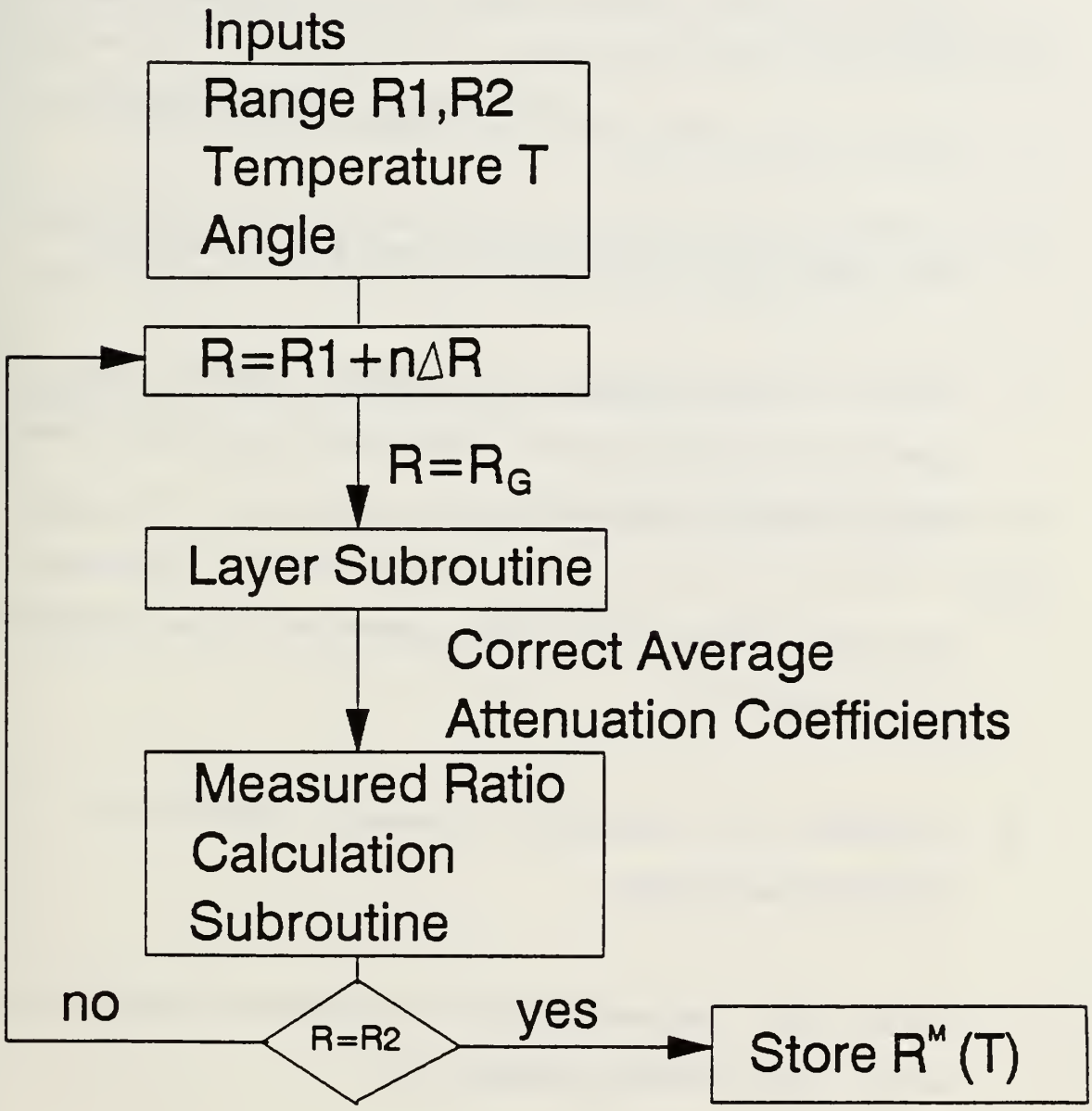

LIST OF REFERENCES

1. Keyes, R.J., and others, *Optical and Infrared Detectors*, Springer-Verlag, 1980.

2. Sze, S.M., *Physics of Semiconductor Devices*, John Wiley & Sons, 1981.

3. Hudson, R.D., *Infrared System Engineering*, John Wiley & Sons, 1969.

4. Johnson, R.B., and Branstetter, E.E., "Integration of Plank's equation by the Laguerre-Gauss quadrature method," *Journal of the Optical Society of America*, v. 64, pp. 1445-1449, November 1974.

5. Johnson, R.B., "Effective radiant sterance computation," *Optical Engineering*, v. 24, pp. 721, August 1985.

6. Nicodemus, F.E., "Normalization in radiometry," *Applied Optics*, v. 12, pp. 2960-2973, December 1973.

7. Horman, M.H., "Temperature analysis from multispectral infrared data," *Applied Optics*, v. 15, pp. 2099-2104, September 1976.

8. Fehribach, J.D., and Johnson, R.B., "Temperature measurement validity for dual spectral-band radiometric techniques," *Optical Engineering*, v. 28, pp. 1255 - 1259, December 1989.

9. Ovrebo, P.J. and Wood, R.C., *Passive Infrared Ranging Device Using Absorption Bands of Water Vapor or Carbon Dioxide,* U.S. Patent 3,103,586, 10 September 1963.

10. Jenness, J.R., Jr. and Shimukonis, F.J., *Apparatus for Passive Infrared Range Finding,* U.S. Patent 3,117,228, 7 January 1964.

11. MacClatchey, R.A., and others, *Optical Properties of the Atmosphere,* Air Force Cambridge Research Laboratories, AFCRL-72-0497, August 1972.

12. Spiegel, M.R., *Mathematical Handbook,* McGraw-Hill, 1968.

13. Kneizys, F.X., and others, *Atmospheric Transmittance/Radiance: Computer Code LOWTRAN 6,* Air Force Geophysics Laboratory, AFGL-TR-83-0187, 1 August 1983.

INITIAL DISTRIBUTION LIST

		No. Copies
1.	Defense Technical Information Center Cameron Station Alexandria, VA 22304-6145	2
2.	Library, Code 52 Naval Postgraduate School Monterey, CA 93943-5002	2
3.	JMSDF Electronic Analysis Center 7-73 Funakoshi-cho Yokosuka-shi, Kanagawa, Japan 238	1
4.	Professor Ronald J. Pieper Naval Postgraduate School Monterey, CA 93943-5000	4
5.	Professor John P. Powers Naval Postgraduate School Monterey, CA 93943-5000	1

Thesis
H57745 Hirakawa
c.1 Passive determination of temperature and range using spectral band measurements of photon emittance.

DUDLEY KNOX LIBRARY
3 2768 00037065 4